Medical Imaging Center and
Transplantation and Liver Surgery Clinic
University of Helsinki
Finland

# MR IMAGING OF THE LIVER: STUDIES ON THE DETECTION AND CHARACTERIZATION OF FOCAL LIVER LESIONS AND LIVER CIRRHOSIS

Kirsti Numminen

*Academic Dissertation*

To be presented, with the permission of the Medical Faculty of the University of Helsinki, for public examination in the Richard Faltin Auditorium at the Surgical Hospital, Kasarmikatu 11-13, Helsinki University Hospital, 19 November 2004, at 12 noon.

Helsinki 2004

***Supervisors***

Professor Krister Höckerstedt

Transplantation and Liver Surgery Clinic, Department of Surgery

Helsinki University Hospital

Docent Pekka Tervahartiala

Medical Imaging Center

Helsinki University Hospital

***Reviewers***

Docent Eija Pääkkö

Department of Diagnostic Radiology

University of Oulu

Docent Tapani Tikkakoski

Department of Radiology

Keski-Pohjanmaa Central Hospital

***Opponent***

Professor Osmo Tervonen

Department of Diagnostic Radiology

University of Oulu

ISBN 952-91-7886-7 (paperpack)

ISBN 952-10-2147-0 (PDF)

Yliopistopaino

Helsinki 2004

## *1. ABSTRACT*

The liver is a common target for a variety of primary malignancies. In the past, mortality following liver surgery was high and curative treatment was seldom available. Early identification of liver metastases provides the opportunity for the success of liver surgery as a therapeutic approach. The resection of metastases is beneficial, especially in patients presenting with liver metastases from colorectal carcinoma. Deciding patients' eligibility for these invasive therapies requires accurate preoperative assessment of the liver tumors, liver parenchyma and the extent of the disease. Differentiation between hemangiomas and other focal liver lesions, such as liver metastases, is also of high clinical importance, especially in the case of patients with a history of a malignancy.

The aim of this thesis was to evaluate the lesion characterization potential of MRI by evaluating several unenhanced MR sequences and the dynamic gadolinium (Gd)-enhanced technique. The diagnostic value of MDCT and MRI in the preoperative assessment of liver tumors was analyzed. The sensitivity and specificity of MRI in diagnosing cirrhosis was also investigated.

In this study, lesion detection was analyzed preoperatively using MRI and MDCT. Thirty-one patients were included in our prospective study. The results showed that triphasic MDCT with thin (2.5 mm) slices and a high-volume, high-concentration contrast material is a very sensitive noninvasive technique in preoperative liver assessment. Both lesion detection and the depiction of lesions in relation to vascular structures were more precise than with MRI. However, both methods had only a limited value in the detection of extrahepatic disease.

The role of MRI in lesion characterization was evaluated in 116 patients. Histological proof of lesion or hemangioma with follow-up was the inclusion criterion. The results indicated that the use of multiple sequences in conjunction with Gd enhancement makes MRI extremely useful in liver lesion classification, while its potential in the assessment of specific diagnosis is only moderate.
Sixty-eight patients were included in the study designed to assess the capability of the true FISP sequence in distinguishing between hemangiomas and malignant liver lesions. The results confirmed that reliable differentiation between hemangioma and malignant liver lesion is possible with the true FISP sequence.

The potential of MRI in diagnosing liver cirrhosis by evaluating the most characteristic MRI features of cirrhosis was also investigated. Study population was 56 patients. All cases were verified histologically. MRI proved to be accurate in diagnosing Child B and C cirrhosis. The most characteristic MRI features of cirrhosis were a large segment one, narrowing of the hepatic veins and signs of portal hypertension, fibrosis and a nodular margin of the liver. MRI was also a sensitive way to detect occult hepatocellular carcinoma.

In conclusion, the studies included in this thesis show that MRI is an accurate method in lesion characterization and in diagnosing liver cirrhosis. The true FISP sequence provides a non-invasive and reliable tool in hemangioma diagnostics. In preoperative liver evaluation, especially in lesion detection; however MDCT performed better than MRI.

***2.CONTENTS***

## *3. LIST OF ORIGINAL PAPERS*

This thesis is based on the following publications.

I Numminen K, Halavaara J, Isoniemi H, Tervahartiala P, Kivisaari L, Numminen J, Hockerstedt K. Magnetic resonance imaging of the liver: true fast imaging with steady state free precession sequence facilitates rapid and reliable distinction between hepatic hemangiomas and liver malignancies. J Comput Assist Tomogr. 27:571-576, 2003.

II Numminen K, Halavaara J, Tervahartiala P, Isoniemi H, Kivisaari L, Palomäki M, Hockerstedt K. Liver tumour MRI: what do we need for lesion characterization? Scand J Gastroenterol. 39:67-73, 2004.

III Numminen K, Isoniemi H, Halavaara J, Tervahartiala P, Mäkisalo H, Laasonen L, Höckerstedt K. Preoperative assessment of focal liver lesions: multidetector CT challenges MRI in lesion detection. Accepted for publication in Acta Radiol.

IV Numminen K, Tervahartiala P, Halavaara J, Isoniemi H, Höckerstedt K. Non-invasive diagnosis of liver cirrhosis: MRI presents special features. Accepted for publication in Scand J Gastroenterol.

The publications are referred to in the text by their Roman numerals.

## *4. ABBREVIATIONS*

| | |
|---|---|
| 3-D | three-dimensional |
| CC | cholangiocarcinoma |
| CNR | contrast-to-noise ratio |
| CTAP | computer tomography during arterial portography |
| EPI | echo planar imaging |
| FISP | fast imaging with steady state free precession |
| FNH | focal nodular hyperplasia |
| FSE | fast spin echo |
| Gd | gadolinium |
| GRE | spoiled gradient echo |
| HASTE | half-Fourier single-shot turbo spin-echo |
| HCC | hepatocellular carcinoma |
| IOUS | intraoperative ultrasonography |
| kV | kilovolt |
| MA | matrix |
| mAs | milliamperesecond |
| MDCT | X-ray computer assisted multidetector tomography |
| MR | magnetic resonance |
| MRI | magnetic resonance imaging |
| NEX | number of excitations |
| NMR | nuclear magnetic resonance |
| PET | positron emission tomography |
| PSC | primary sclerosing cholangitis |
| RARE | rapid acquisition with relaxation enhancement |
| RES | reticuloendothelial system |
| ROI | region-of-interest |
| S1/RL | ratio between transverse diameters of liver segment one and right lobe |
| S1/RLm | modified ratio between transverse diameters of liver segment one and right lobe |
| SE | spin echo |
| SI | signal intensity |
| SNR | signal-to-noise ratio |
| STIR | short inversion time inversion recovery |
| T | tesla |
| TE | time to echo |
| TR | repetition time |
| TSE | turbo spin echo |

## *5. INTRODUCTION*

The approach taken in the treatment of cancer patients relies on knowledge of liver status: high-sensitivity imaging in lesion characterization and detection may prevent unnecessary liver resections or, on the other hand, justify surgery (43, 69). In selected patients presenting with malignant primary or secondary hepatic tumors the potential benefit of surgical resection is well established (24). In general, the outcome in cases of malignant liver tumors is closely related to the stage of the disease. Accurate evaluation of hepatic tumor involvement and possible extrahepatic disease constitutes the basis for appropriate selection and tailoring of treatment for cancer patients. In this process, imaging studies play a pivotal role.

Liver cirrhosis and its complications, especially hepatocellular carcinoma, are major clinical problems that carry a considerable risk of disability and death (174). Traditionally, liver cirrhosis has been diagnosed by liver biopsy. This invasive procedure in cirrhotic patients may run a risk of bleeding complications due to coexisting coagulopathy. Liver resection in cirrhotic patients also carries a high risk of operative mortality (60). Non-invasive tools for the evaluation of liver parenchyma and the detection of tumors are therefore of the utmost importance.

Magnetic resonance imaging (MRI) provides versatile and unique soft tissue contrast, and is thus a powerful tool for evaluating a wide range of liver disorders. Over the past two decades MRI of the liver has experienced unprecedented growth due to advances in hardware and software. At present, MRI is considered to possess greater diagnostic accuracy than computer tomography during arterial portography (CTAP) and helical CT (142, 143, 145, 148). However, the introduction of x-ray computer-assisted multidetector tomography (MDCT) challenges the superiority of MRI (40, 83).

This thesis evaluates the lesion characterization potential of MRI by evaluating several unenhanced MR sequences and the dynamic gadolinium (Gd)-enhanced technique**.** The diagnostic value of MDCT and MRI in the preoperative assessment of liver tumors is also analyzed, and the sensitivity and specificity of MRI in diagnosing cirrhosis is investigated.

## *6. REVIEW OF THE LITERATURE*

### *6.1. History of liver MRI*

The first reported whole-body line-scan experiment was performed during the evening of April 13, 1978. The nuclear magnetic resonance (NMR) image obtained showed the upper abdominal internal organs, including the liver and gall bladder. The thickness of the cross-sectional slice was approximately 4 cm and the scanning time for this one slice was 40 minutes (99). The first case report of a liver tumor diagnosed with NMR was published in January 1981 by Smith et al. (152). In May 1981, Smith et al. (153) were also first to report NMR imaging results for 30 patients with liver disease, including liver cirrhosis and benign and malignant liver tumors. Smith concluded that: "NMR tomographic imaging appears to be an excellent non-invasive technique for the demonstration of various liver conditions. It can demonstrate the presence of malignant and benign liver tumors, obstructive jaundice and inflammatory conditions such as cholecystitis. This short series suggests that there is a large potential for this non-invasive, non-ionizing technique".

Since these early experiences, MRI of the liver has advanced significantly. In 1986, Hennig et al. (61) developed a faster way to acquire a T2-weighted image, and the rapid acquisition with relaxation enhancement (RARE) sequence was launched. Also in 1986, Frahm et al. (45) reported rapid MR imaging using low flip angle pulses. The first clinical study using a 1.5 T unit for hepatic imaging was performed in 1987 by Foley et al. (39). Gadolinium chelates were introduced for clinical abdominal MR imaging in 1984 (19). Superparamagnetic iron oxide was the first tissue-specific contrast agent for the liver (134).

In the 1990's, MRI of the liver progressed significantly with scanner hardware improvements such as high-performance gradient coils and improved body coil design. In addition, the evolution of MRI software with advances in fast imaging techniques, motion artefact suppression, and sequences with greater T1 and T2 weighting has allowed good image quality to be obtained routinely.

### *6.2. Liver MRI scanning technique*

#### *6.2.1. General remarks*

High-quality images of the liver are usually obtained by using a dedicated abdominal coil, preferably a phased array multicoil, which significantly improves the signal-to-noise ratio (SNR) of the image. The improved signal-to-noise ratio afforded by phased array coils allows thinner slices, a smaller field-of-view, and thus higher resolution images to be obtained than with the body coil (18). With fast scanning capabilities, breath-hold imaging can be used to

replace non-breath-hold approaches for improved image quality and can also shorten the examination time (7, 144). Excitation-spoiling chemically selective fat suppression greatly diminishes motion and phase artefacts from respiration and improves the dynamic range of signal intensities of abdominal tissues. Fat suppression improves the signal-to-noise and contrast-to-noise (CNR) ratios of focal liver lesions and is also particularly useful for the visualization of contrast enhancement in regions bordered by fat, such as subcapsular liver parenchyma (8, 96, 138, 139).

### *6.2.2. Sequences*

In abdominal MRI, T1- and T2-weighted sequences are the basic requirement for organ visualization as well as for lesion detection and characterization (114).

#### *6.2.2.1. T1-weighted sequences*

T1-weighted images demonstrate imaging features for various types of liver lesions. Cysts, hemangiomas, and other lesions with a high fluid content are very low in signal. Lesions that are hypovascular or have high fibrous tissue content, such as colon cancer metastases, transitional cell carcinoma metastases, antibiotic-treated abscesses, chemotherapy-treated metastases that are fibrotic, and hepatic fibrosis, are moderately low in signal. Hemorrhagic lesions, including hemorrhagic metastases and liver hemorrhage, high-protein-content lesions, including hepatocellular carcinoma and hepatic adenoma, and melanin-containing lesions, such as melanoma, are high in signal (88).

Spin-echo (SE) or spoiled gradient echo (GRE) sequences are most commonly used to produce T1-weighted images. However, GRE sequences allow the liver to be imaged within a single breath-hold, whereas SE sequences take several minutes to perform and some form of respiratory movement compensation is mandatory to reduce motion artefacts (85). GRE has achieved widespread use as a primary T1-weighted sequence for evaluating the liver (100).

Three-dimensional GRE imaging minimizes vascular pulsation artefacts and permits the acquisition of thinner sections. This technique allows a multiplanar display and is useful for defining hepatic blood vessels (89). Three-dimensional GRE sequences such as volume-interpolated breath-hold examination (VIBE) can produce thin slices with fat saturation and without gaps. This allows MR angiograms to be produced (130). Magnetization-prepared GRE sequences acquire data as a single section technique with each individual section

acquired in less than 2 sec. This sequence is relatively insensitive to artifacts from patient motion and breathing, and has thus been termed breathing-independent (141).

Fast T1-weighted imaging with GRE sequences is the technique most frequently used to obtain images with extracellular contrast agents (56, 130, 139).

***6.2.2.2. T2-weighted sequences***

Normal liver parenchyma has a relatively short T2 time, producing a hypointense signal relative to the spleen, kidneys and most other soft tissues, including tumors. For this reason, T2-weighted images have been considered useful for the detection of focal hepatic lesions that are hyperintense relative to hepatic parenchyma. There is no general opinion on the best T2-techniques and the techniques vary widely depending on equipment and user preferences.

RARE (61) and its modifications fast spin-echo (FSE) and turbo spin-echo (TSE) are basic T2-weighted sequences in liver imaging. These techniques can produce T2-weighted images in less time than conventional spin-echo imaging (20). Fat suppression and respiratory triggering are often combined with the sequences in order to improve the signal-to-noise and contrast-to noise ratios of focal liver lesions (96, 138).

An additional modification of the RARE technique is half-Fourier single-shot turbo spin-echo (HASTE) also known as single shot fast spin echo. The HASTE sequence uses half-Fourier reconstruction to decrease the acquisition time. Because data can be acquired in a very short time, HASTE can provide T2-weighted images during one breath-hold (161). HASTE generates heavily T2-weighted images and is therefore used to differentiate fluid content lesions from solid liver tumors (162); it is also applied in MR cholangiopancreatography (111).

Echo planar imaging (EPI) is another method of obtaining breath-hold T2-weighted scans (135). EPI requires strong and specialized gradients and also a well-shimmed magnetic field with homogeneous fat suppression (47). Short tau inversion recovery (STIR) imaging provides strong image contrast. With STIR, images are generated in which the signal from fat is suppressed while the signal from most pathologies (and fluid) appears bright (151). STIR images can also be obtained with a TSE technique (63) and with breath-hold (36).

***6.2.2.3. True fast imaging with steady state free precession (FISP)***

True FISP is an ultrafast gradient-echo MR sequence in which echo (TE) and repetition times (TR) are kept as short as possible in order to minimize motion and susceptibility artefacts. Image contrast is related to the T2*/T1 ratio. Acquisition time is approximately 10 seconds, allowing scanning to be performed during breath-hold (79, 166). The true FISP sequence has been applied in the MR imaging of the vascular and biliary systems, and in MRI interventions (34, 79).

***6.3. MRI contrast agents***

The need to characterize more accurately different histological types of liver lesions and to detect the full extent of malignant liver lesions has been the main reason for the use of contrast agent (147). The use of contrast agents potentially increases the sensitivity and specificity of liver MRI in numerous pathological conditions by improving morphological information and adding functional information (7). Contrast agents can act as positive or negative enhancers, depending on their nature, concentration, and the imaging pulse sequences (7, 53, 54). Contrast media can be classified into three categories according to their biodistribution: 1) non-specific extracellular contrast agents; 2) agents that are taken up by hepatocytes and excreted to variable extents via the hepatobiliary route; and 3) reticuloendothelial system (RES)-targeted agents (147).

***6.3.1. Non-specific extracellular contrast agents***

Non-specific extracellular contrast agents constitute a group of different types of gadolinium chelates. They have been available since 1984 and have the best documented clinical applications and safety profile. Gadolinium chelates are paramagnetic complexes that increase T1-relaxivity. Tissues where it accumulates are seen brighter in the enhanced T1-weigthed clinical images than in the unenhanced images (172). The standard clinical dosage for the administration of Gd chelates is 0.1 mmol/kg.

***6.3.2. Liver-specific contrast agents***

Liver-specific contrast agents represent a heterogeneous group of compounds in regard to their biodistribution, pharmacokinetic properties, contrast behavior, and most important, their target tissue. With respect to their target tissue, liver-specific contrast media can be divided into hepatocyte-selective and Kupffer's cell-selective contrast agents.

Mangafodipir trisodium (Mn-DPDP) is the oldest hepatocyte-selective contrast agent in clinical use (147). Hepatocyte-selective contrast agents enhance T1 relaxation of normal liver parenchyma. In T1-weighted images, the signal intensity from normal liver and focal hepatic lesions containing hepatocytes increases. Lesions that do not contain hepatocytes remain unchanged (55). Gadolinium-BOPTA and Gd-EOB-DTA are liver-specific contrast agents that can also be used in a way similar to non-specific extracellular agents (21).

RES-specific contrast agents include of superparamagnetic iron oxide particles (SPIO) and ultrasmall superparamagnetic iron particles (USPIO). The presence of the iron particles, which are captured in the Kupffer's cells in the normal liver, increases T2-relaxitivy. In clinical T2-weighted MR images the signal intensity obtained from the normal liver parenchyma decreases. Malignant liver lesions do not contain Kupffer's cells and their signal remains unaltered, and therefore the contrast between malignant lesions and liver increases (53, 134).

Good results has been achieved with liver-specific contrast agents. Ferumoxide-enhanced MR imaging has been proved to be more effective in lesion detection than spiral CT and CTAP (81, 126, 142, 143) and Mn-DPDP has been effective in lesion characterization compared to dual-phase spiral CT (119).

***6.3.3. Dynamic multiphasic liver imaging***

Dynamic imaging after bolus injection of a gadolinium chelate may be the most important component of liver MRI, particularly for characterization of a liver lesion. Optimal dynamic scanning usually depends on the use of the multisection spoiled GRE technique, which allows the entire region of interest to be imaged during a single suspended respiration. Images of the liver are obtained during four phases relative to the injection of the contrast agent: precontrast, arterial (pre-sinusoidal or capillary), portal (sinusoidal), and delayed (interstitial) phases (56, 147).

The arterial phase images are obtained 20-30 seconds from the start of the injection of contrast material. Imaging slightly earlier, when opacification is limited to hepatic arteries only, may be achieved if the injection rate of the contrast material is fast and the sequence is acquired with a very short time (94). In the hepatic arterial dominant phase, gadolinium is present in hepatic arteries and portal veins but absent from hepatic veins. Arterial phase images are important for depicting enhancing hypervascular metastases and hepatocellular carcinomas (109, 159, 177).

Portal-venous phase images are obtained approximately 1 minute after the injection of the contrast material, at which time the delivery of blood by way of the portal-venous system predominates. Because the portal vein supplies 75-80% of the blood flow to the liver, hepatic parenchyma enhances markedly during this phase. The simultaneous delivery of contrast material to the liver lesion will reduce liver lesion contrast for hypervascular tumors. Because most liver tumors are hypovascular relative to the liver parenchyma, they will be visualized as hypointense lesions relative to the enhancing liver in portal-venous phase images (109, 120, 176).

Equilibrium-phase images are obtained 90 seconds to 5 minutes or more after the injection of contrast material. In this time, the injected gadolinium chelate diffuses widely across the capillary endothelium into the interstitial space of the liver and tumors. Most liver lesions become less conspicuous in equilibrium-phase images. However, some tumors with a prominent interstitial space, including cholangiocarcinoma, will accumulate more contrast material than the liver, increasing their conspicuity in delayed images (116). Extrahepatic disease, including peritoneal metastases, is also best visualized in delayed images (93).

### *6.4. Multidetector computer tomography (MDCT) in liver imaging*

MDCT, initially introduced in 1998, has substantially improved the performance of helical CT in several clinical applications, including liver tumor imaging (40, 41, 83). MDCT allows very fast scanning to be performed with thin slices. It can be five to eight times faster than conventional helical CT. A high spatial resolution enables high-quality multiplanar and three-dimensional (3D) reformations to be constructed from the raw data. A high temporal resolution permits multiple precisely defined imaging phases, which is especially useful in hepatic imaging (40, 41, 83). At present, MRI is considered to possess higher diagnostic accuracy than CT during arterial portography and helical CT (142, 143, 145, 148). However, MDCT challenges MRI in liver imaging (40, 133).

### *6.5. Intraoperative ultrasonography*

Intraoperative ultrasonography (IOUS) is regarded as a highly sensitive technique for the accurate staging of liver tumors (44, 136, 167, 173). At present, liver surgery in cases of metastatic and primary malignancies relies on IOUS findings. In a study conducted by Solomon et al. (156), pathological deposits detected by IOUS changed the surgical approach in up to 67% of operations. Surgical palpation and IOUS are routinely used to evaluate the liver before resection, mainly for the detection of occult additional hepatic lesions and to

assess the relationship of tumors to major vessels and extrahepatic structures such as gall bladder and peritoneum (69).

### *6.6. Other imaging modalities*

Positron emission tomography (PET) is a molecular imaging technique that provides images of physiologic processes. In a large meta-analysis by Kinkel (82) FDG-PET was the most sensitive non-invasive imaging modality for detection of hepatic metastases of colorectal, gastric, and oesophageal cancers. However, in detection of hepatic primary malignancies, PET has proved to be insensitive (165). Combined PET/CT devices offer several potential advantages over a PET scanner alone: better quality PET images because of the more accurate correction for attenuation provided by CT, automatic registration of CT (anatomic) and PET (metabolic) information, and shorter imaging times (131).

Ultrasound plays valuable role in the screening of the patients with suspected hepatic disease. Both US and CT are usually the first-line imaging modalities in hepatic diseases (163). Ultrasound also possess high diagnostic performance to identify hepatocellularcarcinoma (165). Ultrasound guided techniques provide commonest interventional techniques for biopsies and drainages (163) and duplex-Doppler technique is a cost-effective modality to evaluate hepatic veins and to obtain hemodynamic information (1).

CTAP was long regarded as the most sensitive method for staging patients with focal liver metastases. However, it is an invasive procedure with attendant risks and it has low specificity (78, 145). Conventional angiography has no role in liver diagnostics today (78). Previously hepatic scintigraphy has been widely used to characterize hemangiomas (33).

### *6.7. Liver diseases*

#### *6.7.1. Benign hepatic tumors*

Benign tumors of the liver are classified pathologically by their cell origin. Lesions of epithelial origin include hepatic cyst, focal nodular hyperplasia (FNH), hepatocellular adenoma, cystadenoma and biliary hamartoma. Lesions of mesenchymal origin include hemangiomas, angiomyolipomas, and lipomas (51). In most cases typical MR imaging characteristics can be observed.

#### *6.7.1.1. Hepatic cyst*

Hepatic cysts are common, and most are asymptomatic. Hepatic cysts form as a result of cystic dilatation of aberrant bile ducts in the liver. These hepatic ducts are incompletely developed and do not connect with normal bile ducts (73). MRI shows the cysts to be hypointense in T1-weighted and hyperintense in T2-weighted images. Simple cysts do not enhance and have a homogeneous and well-defined appearance (115).

#### *6.7.1.2. Hepatic hemangioma*

Hepatic hemangiomas are the most common benign solid liver tumors, with a reported incidence of up to 20% (76). Almost invariably, they are asymptomatic and therefore detected only incidentally during routine abdominal ultrasound examinations (108). Histopathologically, cavernous hemangiomas are well-defined, blood-filled tumors with vascular channels lined with epithelium, separated by fibrous septa. Calcification, internal hemorrhage, thrombosis, and extensive fibrosis may occasionally be present (110).

Hemangiomas generally have moderately low signal intensity in T1-weighted images and high signal intensity in T2-weighted images with a homogeneous pattern. They maintain high signal intensity in heavily T2-weighted images (104). Hemangiomas have three basic enhancement patterns: uniform enhancement on arterial phase scans, typically seen in hemangiomas 1 cm in size or smaller, nodular peripheral enhancement with centripetal filling on sequential sequences, and nodular peripheral enhancement with centripetal filling in with persistence of a non-enhancing central scar (140).

#### *6.7.1.3. Focal nodular hyperplasia*

FNH accounts for approximately 8% of all primary hepatic tumors in western world (51). Most FNHs are seen in women (80%-95%) in the third to fifth decades of life. FNH is thought to arise as a localized hepatocyte response to an underlying congenital vascular malformation (168). The signal intensity of both T1- and T2-weighted images may be close to that of normal liver parenchyma (103). If a central scar is present, it is hyperintense in T2-weighted images. With intravenous gadolinium injection, FNH displays a characteristic pattern of marked, uniform enhancement in arterial-phase images obtained immediately after the bolus administration. In the subsequent portal-venous phase, the lesion rapidly fades, becoming isointense or only mildly hyperintense relative to liver parenchyma (97).

#### *6.7.1.4. Hepatic adenoma*

Liver cell adenomas are rare benign tumors associated in particular with the use of oral contraceptives or anabolic steroids. They can also occur in patients with metabolic disorders such as diabetes mellitus, galactosemia, and glycogen storage disease (80, 132, 154). The incidence of adenomas in patients with long-term oral contraceptive use is approximately 3 to 4 cases per year per 100,000 population (132). Histologically, adenomas are composed of cords of hepatocytes, large amounts of fat and glycogen. There are no bile ductules, portal venous tracts, or terminal hepatic veins (51). Adenomas are usually vascular-rich tumors and have a propensity to outgrow their vascular supply, resulting in hemorrhage and necrosis, and large ones may occasionally rupture. The MR imaging appearance can be variable and non-specific. Most have a heterogeneous appearance correlating with the amount of fat and hemorrhage (122). Adenomas often enhance strongly in arterial phase images (25). Differential diagnosis with respect to hepatocellular carcinomas can be difficult if adenomas contain fat or hemorrhage (108). Because of the risk of hemorrhage, adenomas may require surgical treatment (106, 108). Malignant transformation is rare (50).

### *6.7.2. Malignant liver tumors*

#### *6.7.2.1. Liver metastases*

Metastatic disease is the most common cause of malignant liver lesions, outnumbering primary hepatic neoplasm by 18 to 40 times (5, 51). Up to 75% of primary tumors drained by the portal venous system (pancreas, large bowel, small intestines and stomach) will have metastatic involvement at some stage of the disease. About 10% of these will have a solitary liver metastasis. This figure is much lower for other tumors such as those of the breast and the lung (71). Metastases are classified as hypo- or hypervascular. The majority of liver metastases are hypovascular, usually originated from gastro-intestinal tract and from breast and lung carcinoma. (120). Hypovascular metastases are best depicted in portal-venous phase images. These metastases receive minimal blood supply from the hepatic artery. During the portal-venous phase, the liver parenchyma demonstrates marked enhancement while hypovascular metastases show only minimal enhancement, producing the greatest difference in liver-lesion signal intensity (109, 120, 175). In arterial phase images, rim-enhancement has been reported to be highly specific for hypovascular metastases (98). Hypervascular metastases are supplied by the hepatic artery and enhance rapidly after injection of gadolinium chelates. Typical hypervascular liver metastases arise from renal and breast carcinoma, islet cell tumors, melanoma, and sarcoma (120). Thus, in arterial phase images, hypervascular metastases will show marked enhancement against a background of minimally

enhancing liver parenchyma (87, 159). In later phases the contrast agent within the tumor will wash out and the tumor will become hypo-or isointense to liver parenchyma.

In T2-weighted MR images, metastases are usually mildly hyperintense relative to the liver. However, some metastases, particularly liver metastases from breast and colon carcinomas and metastases from neuroendocrine malignancies and chemotherapy-treated lesions, may have a high signal intensity in T2-weighted images (146, 159). In unenhanced T1-weighted images they are hypointense except for occasional melanoma metastases, which may appear bright (88) and demonstrate a low signal in T2-weighted images due to the presence of melanin (90).

#### *6.7.2.2. Hepatocellular carcinoma*

Hepatocellular carcinoma is the most common primary malignancy of the liver. Patients who are carriers of chronic hepatitis B or C virus infection, or those who have cirrhosis caused by alcohol or hemochromatosis are at greater risk of developing HCC (71). The fibrolamellar variant of HCC, however, has usually no association with cirrhosis. HCC arises from dysplastic nodules (35). Dysplastic nodules progress from low-grade dysplastic nodules to high-grade dysplastic nodules. High-grade dysplastic nodules may develop microscopic foci of HCC that then enlarge to become a frank malignant HCC. HCC can appear as a solitary or multifocal liver mass or as a diffuse infiltrative tumor. Portal-vein invasion and intrahepatic metastases and tumor capsule are characteristic features of HCC (38).

HCC shows a highly variable appearance in both T1- and T2-weighted images (46, 175). Hyperintense regions within HCC in T1-weighted images reflect the presence of fat, copper, or protein. On T2-weighted images HCCs are generally hyperintense (102), although well-differentiated tumors may be isointense to liver parenchyma (64, 118). A mosaic pattern is seen if the tumor is larger than 3 cm (74). HCCs are mainly nourished by the hepatic artery. They are usually greatly enhanced in arterial dominant–phase images. The enhancement is often homogeneous in tumors less than 2 cm in diameter and heterogeneous in tumors larger than 2 cm. However, a well-differentiated HCC often shows minimal arterial–phase enhancement (175). There is overlapping between imaging features of regenerative, dysplastic and HCC nodules. Especially signal intensity of dysplastic nodules overlaps significantly with those of small HCCs (64, 84). Also enhancement pattern of dysplastic nodules can be similar to small HCCs. In difficult cases only follow up or biopsy can verify the diagnosis (70).

***6.7.2.3. Cholangiocarcinoma***

Cholangiocarcinoma (CC) arises from bile duct epithelium and is the second most common primary malignancy, accounting for 8.2% of all primary malignant hepatic neoplasms (71). An increased incidence of CC has been associated with a variety of predisposing factors such as primary sclerosing cholangitis, cystic biliary disease, intrahepatic ductal calculi, and congenital biliary atresia.

In T1- and T2-weighted images, cholangiocarcinoma is hypo- and hyperintense, respectively. A small central type of cholangiocarcinoma can be obscured by dilated bile ducts. After injection of gadolinium, CC displays a characteristic pattern of slow, gradual enhancement. The delayed enhancement of CC in equilibrium-phase images is considered to be a characteristic feature (158).

Hepatic angiosarcoma, biliary cystadenocarcinoma, epitheloid hemangioendothelioma, lymphoma and nonvascular sarcomas are rare primary liver malignancies.

***6.7.3. Liver cirrhosis***

Liver cirrhosis is characterized by the presence of extensive fibrosis and innumerable regenerative nodules replacing the normal liver parenchyma. These features represent the final common pathway of chronic liver injury due to a variety of causes. The process is initiated by parenchymal necrosis, followed by connective tissue deposition, nodular hepatocyte degeneration, and distortion of the lobular and vascular hepatic architecture (15). In Europe the most common etiology for cirrhosis is alcohol (26). The prevalence of other chronic liver disorders such as viral hepatitis, primary biliary cirrhosis, primary sclerosing cholangitis, and autoimmune hepatitis varies considerably in different countries (12, 101). The Child-Pugh scoring system is used to assess the severity of liver cirrhosis. The Child-Pugh grade is related to bilirubin, albumin, and prothrombin values and to the presence or absence of hepatic encephalopathy and ascites (table 1)(149). The clinical manifestation of cirrhosis is related to loss of hepatocellular function and complications of portal hypertension (137). Traditionally, cirrhosis has been established invasively by liver biopsy, although cirrhotic patients often suffer from coagulopathy (137). Liver cirrhosis is also associated with a markedly increased risk of hepatocellular carcinoma (71, 169). The role of radiology in the evaluation of cirrhosis is primarily to characterize the morphologic manifestations of the disease, evaluate the hepatic and extrahepatic vasculature, assess the effects of portal hypertension, and detect hepatocellular cancer (16). The typical radiological manifestations of the liver cirrhosis are ascites, spenomegaly, portosystemic shunt vessels, large segment one,

nodularity of the liver, shrinkage of the right lobe (16) and large gall blader fossa (66). Liver transplantation is nowadays widely accepted as a therapeutic option for patients with terminal liver failure (9).

| **Criteria assessed** | **Points scored for increasing abnormality** | | |
|---|---|---|---|
| | 1 | 2 | 3 |
| encephalopathy (grade) | none | 1-2 | 3-4 |
| ascites | absent | slight | moderate |
| serum bilirubin (μmol/l) | <35 | 35-50 | >50 |
| serum albumin (g/l) | >35 | 35-28 | <28 |
| prothrombin time (s) | 1-4 | 4-10 | >10 |
| total score | 5-6 | 7-9 | 10-15 |
| **Child´s grade** | A | B | C |
| **overall mortality in Pugh`s series (%)** | 29 | 38 | 88 |

Table 1 Child-Pugh scoring system

***6.8. Treatment of malignant liver tumors***

The majority of liver resections are performed for metastatic colorectal cancer. One-third of colorectal carcinoma patients develop liver metastases, 20% of which are confined to the liver. Approximately a quarter of these 20% may be candidates for liver resection. The ultimate indications for liver surgery vary between different units. Potential candidates for a liver resection must have no evidence of extrahepatic spread of the disease and have no comorbid conditions to preclude a major operative procedure (60, 71). The predictors for a good outcome are a surgical margin of at least 1 cm, four or less liver lesions, a serum low carcino-embryonic antigen level and the small size of the metastasis (17, 24, 42, 43). A long-term survival rate of 25%-39% has been reported after curative resection, whereas the rate is only 2% after medical therapy or no therapy (42, 60, 164). Previously 5-fluorouracil has been the commonest cytotoxic agent for systemic chemotherapy. Improved results have been achieved after combining fuorouracil/leucovorin with bevacizumab, which is a monoclonal antibody to vascular endothelial growth factor (72). Very promising results have been seen

with more a modern chemotherapeutic regimen comprising irinotecan, oxaliplatin and capecitabine, which is an oral formula (14).
The only curative treatment for HCC is surgical resection or liver transplantation. However, HCC is mostly associated with cirrhosis and therefore usually beyond the reach of resection. On the other hand, resection of a cirrhotic liver is associated with relatively high morbidity and mortality (86, 171, 178). Death is usually caused by liver failure or severe dysfunction or finally multiorgan failure. The 5-year survival of patients resected for HCC is about 50% (92, 127, 178). The favorable determinants of survival include no vascular invasion or extrahepatic disease, asymptomatic status, and a solitary and encapsulated tumor less than 5 cm size. A 1 cm tumor-free margin is an even more important determinant of prognosis in HCC than in colorectal cancer metastases (22, 127, 150). Fibrolamellar HCC is a rare variant of HCC. It is not associated with cirrhosis, and the surgical survival rate after 10 years can be up to 70% (60, 71).

The alternative therapeutic techniques for surgical treatment include chemoembolization, percutaneous ethanol injection therapy, cryotherapy, microwave ablation and interstitial laser coagulation. At the moment radio-frequency ablation is considered to be the most promising technique (48). The main indications for these local ablative techniques is poor liver function with insufficient liver reserve after liver resection or comorbid conditions (23). Although a 3-year-survival rate as high as 46% has been reported (155), patients with potentially resectable tumors should be treated using hepatic resection, which is still considered to be the gold standard therapy (105).

## *7. AIMS OF THE STUDY*

The aims of the present study were

1. To study the diagnostic value of MDCT and MRI in the preoperative assessment of liver tumors in relation to lesion detection, the lesion's vascular proximity and extrahepatic disease (study III).

2. To determine the potential of MRI in liver lesion characterization by using tumor histology as the gold standard (study II).

3. To analyze the potential of the true FISP sequence in distinguishing between hemangiomas and malignant liver lesions (study I).

4. To investigate the sensitivity and specificity of MRI in diagnosing liver cirrhosis by evaluating the most characteristic MRI features of cirrhosis. Co-incidental HCC was also analyzed (study IV).

## *8. MATERIALS AND METHODS*

### *8.1. Patient population*

A total of 180 patients were examined in this investigation. 91 patients were same in different publication. In the retrospective studies (I, II and IV) the inclusion criteria were either histological proof of a lesion and liver parenchyma or a hemangioma with a follow-up. In study III, 31 consecutive patients eligible for hepatic surgery during 2002 were included. All investigations were made in a hospital orientated to hepatic surgery. This influenced to patient selection. The patient characteristics are summarized in Table 2.

| **Study** | I | **II** | III | **IV** |
|---|---|---|---|---|
| **Patients** | 68 | 116 | 31 | 56 |
| female | 38 | 70 | 14 | 28 |
| male | 30 | 46 | 17 | 28 |
| female, mean age, (range) | 55.5 (35-76) | 53.2 (25-78) | 58.3 (29-69) | 52.3 (28-75) |
| male, mean age, (range) | 56.2 (35-82) | 56.7 (35-77) | 57.4 (26-75) | 57.6 (35-78) |
| **Histology (n=patients)** | | | | |
| HCC | 10 | 17 | 3 | 13 |
| cholangiocarcinoma | 7 | 12 | 3 | 5 |
| gall bladder carcinoma | 2 | 6 | | |
| angiosarcoma | 1 | 1 | | |
| colorectal metastases | 17 | 24 | 20 | 1 |
| other metastases | 8 | 16 | 2 | |
| no tumor | | | | 28 |
| hemangioma | 23 | 23 | | 2 |
| FNH | | 11 | 1 | 5 |
| adenoma | | 3 | 1 | 1 |
| other benign liver lesions | | 3 | 1 | |
| mean diameter of malignant lesions (cm) | 3.9 (2-12) | 5.1 (1-15) | 3.0 (1-10) | |
| hemangiomas | 3.1 (1-14) | | | |

Table 2. Patient characteristics in studies I-IV

Study I consisted of sixty-eight patients. The hemangioma group contained 23 patients with 45 hemangiomas. There were 17 women (age range 35-75 years, mean 48.5) and 6 men (age range 35-69 years, mean 54.5). Histological proof was obtained from 14 hemangiomas. The remaining 31 hemangiomas demonstrated typical T2-signal behavior and characteristic fill-in enhancement patterns during dynamic gadolinium-enhanced MRI. None of the hemangiomas showed progression during a mean follow-up time of 16 months (range, 6-24 months). The mean diameter of the hemangiomas was 3.1 cm (range 1.0-14.0 cm). The patient group with malignant liver lesions contained 21 women (age range 36-76 years, mean 62.4) and 24 men (age range 43-82 years, mean 57.9) with 51 focal lesions. There were a total of 31 metastases. 19 metastases (17 patients) originated from the colorectum and 12 metastases (8 patients) were of other origin. Additionally, there were 10 cases of hepatocellular carcinomas, seven cholangiocarcinomas, two infiltrating gall bladder carcinomas, and one angiosarcoma. The mean diameter of the malignant liver lesions was 3.9 cm (range 2.0-12.0 cm). All malignant lesions were histologically verified.

Study II involved a total of 116 focal liver lesions in 116 patients. The patient group with 76 malignant liver lesions included 38 men (age range 45-86 years, mean 60.2) and 38 women (age range 36-84 years, mean 62.7). The malignancies consisted of metastases (n=40), hepatocellular carcinomas (n=17), cholangiocarcinomas (n=12) and gall bladder carcinomas (n=6), and there was one case of angiosarcoma. The metastases originated from the colorectum (n=24), breast (n=4), pancreas (n=4) and gall bladder (n=2), and there were also one metastasis each from a teratoma, melanoma, leiomyosarcoma, hemangiopericytoma, kidney and carcinoid tumor. The mean size of the malignancies was 5.1 cm (range, 1.0-15.0 cm). The group of patients with 40 benign focal liver lesions included 8 men (age range 25-60, mean age 53.2) and 32 women, (age range 23-80, mean age 43.6). The benign hepatic lesions consisted of hemangiomas (n=23), focal nodular hyperplasias (n=11), adenomas (n=3), cystadenoma (n=1), hemangioendothelioma (n=1) and a complicated cyst. The mean size of the benign liver lesions was 4.7 cm (range, 1.0-15.0 cm).

In study III, 31 patients were preoperatively imaged. There were 17 men (age range 26-75 years, mean 57.4) and 14 women (age range 29-69 years, mean 58.3). Twenty patients had hepatic metastases from colorectal cancer, one patient from breast carcinoma and one patient had metastases from a clear cell sarcoma originating from the kidney. Three patients suffered from hepatocellular carcinoma and three had cholangiocarcinoma. Additionally, there was one case of atypical focal nodular hyperplasia, one adenoma and an old granulomatous

tuberculous lesion (the patient had a history of renal carcinoma). Eleven patients with colorectal metastases received chemotherapy before surgery. All lesions were histologically verified. The mean diameter of the lesions was 3.0 cm (range 1-10 cm).

Study IV comprised 56 patients. The cirrhosis group consisted of 30 patients. There were 18 men (age range 35-68 years, mean 52.7), and 12 women (age range 30-75 years, mean 56.3). The etiology of liver cirrhosis was alcohol (n=8), primary biliary cirrhosis (n=7), primary sclerosing cholangitis (PSC) (n=5), autoimmune hepatitis (n=3), post-viral hepatitis (n=2) and cryptogenic (n=5). Ten patients had coexisting HCC and one patient had a hemangioma. Seven patients were in Child-Pugh class A, 18 in class B and five in class C. The control group included 26 patients, comprising 16 women (age range 28-72 years, mean 48.2) and 10 men (age range 42-78 years, mean 58.9). Histological findings from the liver showed normal liver parenchyma (n=5), nearly normal parenchyma (n=2), mild hemosiderosis (n=1), steatosis (n=13), mild fibrosis (n=3), and necrosis (n=2) within the liver. The main diagnoses of these patients were cholangiocarcinoma (n=5), focal nodular hyperplasia (n=5), hepatocellular carcinoma (n=2), fibrolamellar HCC (n=1), hemangioma (n=2), adenoma (n=1), colorectal metastasis (n=1), acute liver failure (n=2), autoimmune hepatitis (n=2), chronic hepatitis of unknown etiology (n=1) and PSC (n=4). PSC cases were diagnosed by endoscopic retrograde cholangiography.

***8.2. MR imaging***

In all studies MR imaging was performed with a clinical 1.5 T system (Magnetom Vision, Siemens, Erlangen, Germany). A dedicated phased-array body coil was used. Fat-suppressed T2-weighted HASTE with TR = 4.2 ms, TE = 59 ms, slice = 5-6 mm, matrix (MA) = 128 x 256, number of excitations (NEX) = 1, fat-suppressed T1-weighted fast low angle shot (2D-FLASH) TR = 85.6, TE = 4.1, slice = 5 mm, average MA = 192 x 256, NEX = 2 and true FISP TR = 6.3, TE = 3.0, slice = 5mm, average MA = 263 x 350, NEX=1 sequences were acquired. Dynamic Gd-enhanced MR imaging using the fat-suppressed T1-weighted sequence was subsequently performed in the arterial and portal venous phases. The imaging parameters were kept identical. A power-injector was used for the gadolinium injections (Magnevist, Schering AG, Germany, dose 0.1 mmol/kg body weight; injection rate 2 ml/s). All acquired sequences were performed in the axial plane in breath-hold. Liver-specific contrast agent agents were not included in our clinical routine.

***8.3. MDCT imaging***

In study III, a triphasic contrast-enhanced MDCT study was performed with a four-channel scanner (LightSpeed, General Electric Medical Systems, Milwaukee, WI). A 120-140 kV tube voltage and 300-380 mAs current were used. After contrast agent injection at 5 ml/s (150 ml, Ultravist 370 mgI/ml, Schering, Berlin, Germany), bolus-triggered scans in the early arterial, late arterial and portal venous phases were acquired (approximately 20, 40 and 65 seconds after injection). A collimation of 5 mm was used in the arterial phases of imaging, and a collimation of 2.5 mm in the portal venous phase scanning. All phases of imaging were performed with a 0.8 sec gantry rotation, a pitch of 6 and a 15 mm table feed with each gantry rotation.

***8.4. Intraoperative ultrasonography***

In study III, IOUS was performed by both a radiologist and a surgeon in a systematic fashion using GE Logiq 700 equipment with a dedicated 7.5 MHz intraoperative probe (General Electric Medical Systems, Milwaukee, WI). In the department of liver surgery and transplantation IOUS has been used for 15 years.

***8.5. Image analysis***

In studies I, II and IV, the images were evaluated retrospectively and in study III prospectively. In none of the investigations was clinical data available to the readers. The images were analyzed separately in studies I and II and as a consensus reading in studies III and IV by two readers.

In studies I and II, the readers were asked to determine whether the lesion was benign or malignant, and to propose a specific diagnosis. The determination was assessed on the basis of lesion signal characteristics, enhancement patterns and morphology. After the film reading in study I, the principal investigator measured the lesion CNR values and evaluated lesion borders from the true FISP images. For the calculations, signal intensities (SI) were obtained from the lesions and from normal liver parenchyma using the standard region-of-interest (ROI) technique. The largest possible ROI covering the entire lesion was chosen and its periphery was excluded to avoid the partial volume effect. The SI value of the liver was obtained from the vicinity of the respective lesion, and the background noise was determined using a ROI in the phase-encoding direction ventral to the patient. CNR was defined as ($SI_{lesion} - SI_{liver}$) divided by the standard deviation of the background noise.

In study III, the sizes and numbers of liver lesions as well as the hepatic segments involved were recorded for the solid lesions. Couinaud's anatomical description of eight liver segments (27) for lesion localization was used. Coexisting benign lesions such as hemangiomas and cysts were also noted. The anatomical proximities of the lesions to the inferior vena cava or hepatic veins, hepatic hilum, and to the main portal branches were assessed. For this purpose, a scale for the lesion's proximity of less than 1 cm or more than 1 cm was used (17). Benign or suspected malignant lymph nodes were scrutinized and the possibility of other extrahepatic involvement such as infiltration through the hepatic capsule or peritoneal metastases was considered.

In study IV, the readers determined the following liver parameters: enlargement of segment one, atrophy of the right lobe, enlargement of the hilar periportal space, a nodular liver surface, liver nodules, signs of iron deposition, signs of fibrosis (regions of low signal intensity in unenhanced T1-weighted images and increased signal intensity in T2-weighted images), an expanded gall bladder fossa (67), presence of ascites, signs of portal hypertension (enlargement of spleen, portosystemic collaterals), and narrowing of the hepatic veins and vena cava (a subjective criteria was used). The ratio between the transverse diameters of liver segment one and the right lobe (S1/RL) determined by Harbin (59) was measured. Also, the modified ratio between segment one and the right lobe (S1/RLm) as described by Awaya (4) was calculated. Hepatocellular carcinoma or other possible neoplasms were scrutinized. The determination of HCC was assessed on the basis of lesion signal characteristics, enhancement patterns and morphology Finally, readers determined whether the patient had a cirrhotic or a non-cirrhotic liver.

***8.6. Statistical analysis***

In study I, the statistical difference between the true FISP, HASTE, and Gd-enhanced imaging in diagnosing hemangiomas was assessed using the McNemar test. The statistical difference between the CNR values obtained with the true FISP and HASTE was calculated using a two-tailed unpaired t-test. The McNemar test was used in study II to calculate the statistical difference between the collection of sequences and the individual sequence, both in lesion classification and in assessing a specific diagnosis. The McNemar test was also used in study III to measure the statistical significance of the sensitivities between the different imaging modalities. In study IV, the $^2$-test was used to evaluate the statistical significance of the difference in imaging findings between the cirrhosis and control groups. The statistical difference of S1/RL and S1/RLm measurements between the cirrhosis and control groups was

determined using the two-tailed unpaired t-test. A $p < 0.05$ was considered to indicate a statistically significant difference in all tests. In studies I and II, interobserver variances were determined using kappa statistics. A kappa value greater than 0.81 is considered excellent, a value of 0.61-0.80 substantial, 0.41-0.60 moderate, 0.21-0.40 fair, and 0.01-0.20 slight.

## *9. RESULTS*

### *9.1. Lesion detection by MRI, MDCT and IOUS (study III)*

A total of 45 solid lesions from 31 patients were detected by IOUS and palpation during operations. Tumors were verified either by biopsy or from explants histopathologically. From the 45 solid liver tumors, MDCT revealed 43 lesions (96%) and MRI 35 lesions (78%). The differences in the sensitivity of lesion detection between MDCT and MRI were statistically significant (p=0.008). Between MDCT and IOUS no statistically significant difference was detected (p=0.25). However, the differences in sensitivity between MRI and IOUS were statistically significant with a p value of 0.001. All cysts and the solitary hemangioma were detected by IOUS, MRI and MDCT.

### *9.2. Detection of extrahepatic disease and assessment of vascular proximity*

During the operation, metastatic lymph nodes were found in six of 31 patients. In one case lymph nodes were considered potentially metastatic in MDCT as well as in MRI. Capsular infiltration (n=5), peritoneal metastases (n=3) and mesenteric metastases (n=2) were detected by IOUS in seven patients. This extrahepatic involvement was suspected in two cases in MDCT and in one case in MRI. Assessment of the lesion in relation to hepatic vessels, to inferior vena cava and to portal branches was correct in 98% of measurements by MDCT and in 87% by MRI. This difference was statistically significant (p=0.002).

### *9.3. Lesion characterization by MRI (study II)*

#### *9.3.1. Lesion classification*

Lesion classification into benign or malignant tumors was correctly assessed by reader 1 with the true FISP, HASTE, unenhanced T1- and Gd-enhanced T1-weighted sequences in 70%, 72%, 58%, and 79% of cases, respectively. The respective figures for reader 2 were 75%, 76%, 66%, 81%. When all sequences were evaluated collectively, correct characterization of lesions as benign or malignant was achieved in 83% by reader 1 and in 89% of cases by reader 2. The reading of all sequences collectively was superior to the best individual sequence (Gd-enhanced T1-weighted sequence), demonstrating statistical significance

(p=0.02). The difference between the Gd-enhanced T1-weighted sequence and HASTE also showed statistical significance with a p-value of 0.02. In lesion classification, interobserver variance varied from 0.22 to 0.38, indicating fair agreement. The results of lesion classification are presented in Figure 1.

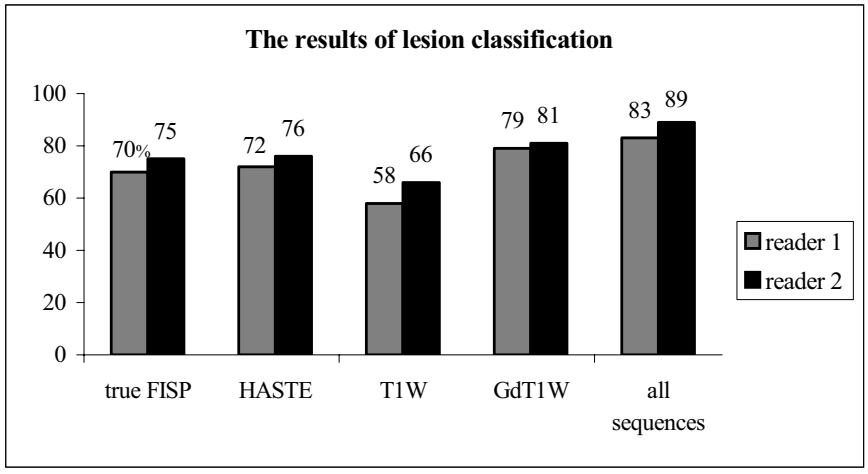


Figure 1. Histogram demonstrating the rates of correct lesion classification into benign or malignant with different MRI techniques. The number of lesions was 116, of which 107 were verified histologically and 9 hemangiomas had a follow up. The figures shown are percentages.

***9.3.2. Specific diagnosis***

Collective evaluation of all sequences gave the best result in terms of assessment of specific diagnosis. Reader 1 correctly diagnosed 60% of cases and reader 2 71%. There was no statistically significant difference between best individual sequence (Gd-enhanced T1-weighted sequence) and the collective evaluation (p=0.06). However, there was a statistically significant difference between Gd-enhanced T1-weighted and T2-weighted sequences, the p-value being 0.03.

Reader 1 reached the correct specific diagnosis with the true FISP, HASTE, unenhanced T1- and Gd-enhanced T1-weighted sequences in 50%, 56%, 41%, and 59% of cases, respectively. The corresponding figures for reader 2 were 53%, 58%, 50% and 65%. The kappa values in

the assessment of specific diagnosis varied from 0.52 to 0.62, indicating moderate agreement. The results for the assessment of specific diagnosis are presented in Figure 2.

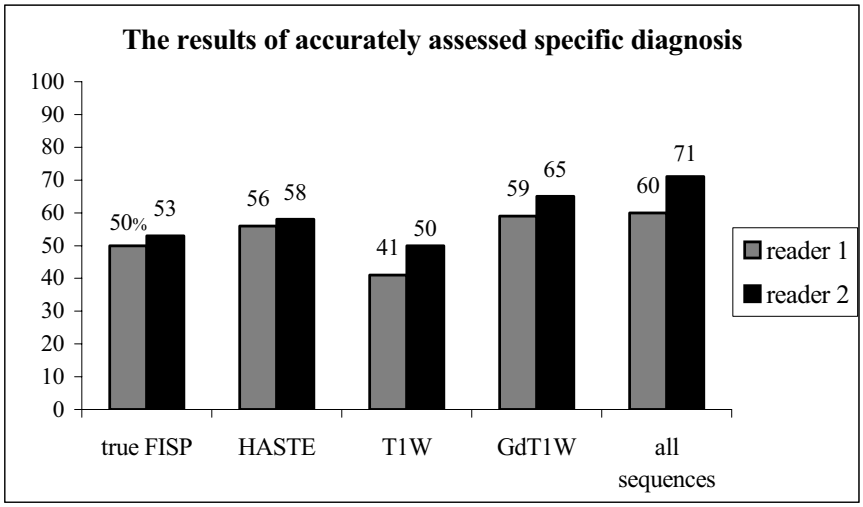


Figure 2. Histogram demonstrating the rates of correct specific diagnoses with different MRI techniques. The number of lesions was 116, of which 107 were verified histologically and 9 hemangiomas had a follow up. The figures shown are percentages.

***9.4. Differentiation between hemangiomas and malignant liver lesions by MRI (study I)***

With the true FISP sequence, a correct hemangioma diagnosis was achieved in 96% and in 89% of cases by readers 1 and 2, respectively. The kappa value was 0.65. With the HASTE, a correct diagnosis was reached in 89% and in 80% of cases by readers 1 and 2, respectively. The kappa value was 0.33. There was no statistically significant difference between true FISP and HASTE in diagnosing hemangiomas (p=0.125). With the unenhanced T1-weighted sequence, only 24%, (reader 1) and 49%, (reader 2) of hemangiomas were correctly diagnosed. Gd enhancement considerably increased the rate of accurate classification: for readers 1 and 2 they were 78% and 82%, respectively. There was no statistically significant difference between true FISP and Gd-enhanced MRI in diagnosing hemangioma (p=0.06). The results of the reader analysis are summarized in Figure 3.

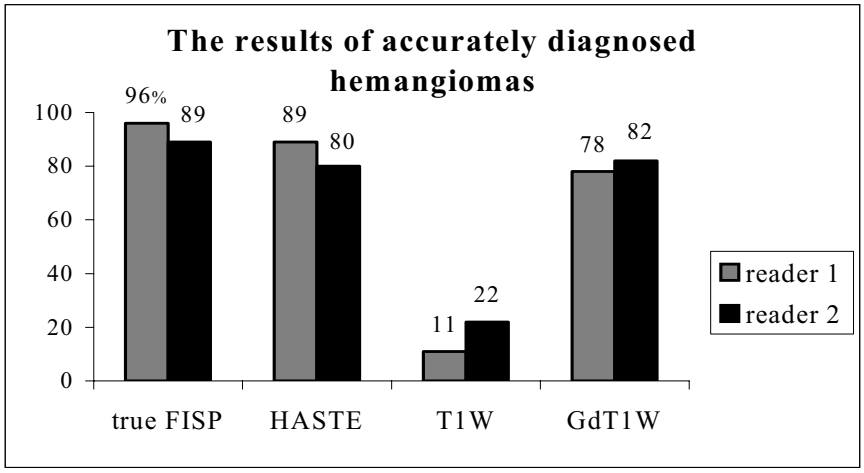


Figure 3. Independent reader analysis with different MR imaging sequences showing correct classification of all hemangiomas (n=45). The figures are shown in percentages.

The calculated specificity of the true FISP sequence was 100% for reader 1 and 98% for reader 2. Twenty-seven of the 45 hemangiomas were 1 to 2 cm in diameter. Both readers correctly diagnosed this subgroup of small hemangiomas better with true FISP than with

HASTE or with dynamic Gd-enhanced MRI. The results for these small lesions are summarized in Table 3.

| | true FISP | HASTE | Gd- T1W |
|---|---|---|---|
| Reader 1 | 25 (93%) | 22 (81%) | 17 (63%) |
| Reader 2 | 23 (85%) | 19 (70%) | 20 (74%) |

Table 3. Independent reader analysis with different MR imaging sequences showing correct classification of small hemangiomas (1-2 cm in diameter, n| 27).

The mean CNR value for the hemangiomas was 21.2, SD 9.2, and for malignant lesions 4.9, SD 3.9. The difference in the CNR values between the two lesion groups was statistically highly significant ($p<0.0001$). There was only a slight overlap in the CNR values between the lesion groups with only two malignant lesions, demonstrating CNR values (11.0 and 21.0) similar to those for hemangiomas (Figure 4).

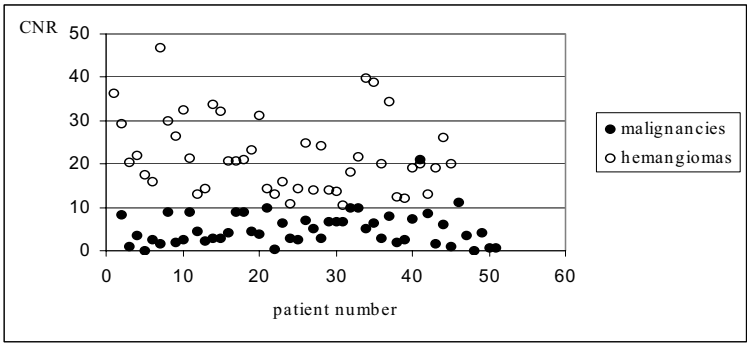


Figure 4. CNR values for hemangiomas (n=45) and malignant liver lesions (n=51). The graph shows the calculated CNR values of the various liver lesions. Hepatic hemangiomas demonstrate significantly higher CNRs than liver malignancies ($p<0.0001$).

### *9.5. Liver cirrhosis (study IV)*

The overall sensitivity and specificity of MRI in the diagnosis of liver cirrhosis were 87% and 92%, respectively. The most characteristic imaging findings suggestive of liver cirrhosis were enlargement of segment one (83% of cases) and narrowing of the hepatic veins (83% of cases). The respective numbers in the control group were 11% and 23%. These differences showed statistical significance (p-values < 0.0001). Enlarged spleen and liver fibrosis were found in 77% of cases. A nodular surface of the liver was detected in 70% of patients with cirrhosis. Regenerative nodules, enlargement of the hilar periportal space, ascites and atrophy of the right lobe were observed in 67%, 60%, 57%, and 50% of cases, respectively. Portosystemic collaterals, expanded gall bladder fossa and iron depositions were detected in 47%, 37%, 23% of patients, respectively.

All co-incidental HCC deposits (n=10) and the solitary hemangioma were correctly diagnosed in the cirrhosis group. However, there was one false positive diagnosis of HCC. The lesion proved to be a large regenerative nodule, six core needle biopsies were taken from lesion.

In the control group, enlargement of the spleen was detected in three patients (11%). Enlarged hilar periportal space, narrowing of hepatic veins, ascites and fibrosis were observed in 30%, 23%, 27%, and 15% of patients, respectively. In two patients (8%), regenerative nodules and a nodular surface of the liver were noted. In one case (4%), an expanded gall bladder fossa was found. In the control group neither iron depositions, atrophy of the right lobe nor portosystemic collaterals were found in any patients. Both cases of HCCs were detected. There was a statistically significant difference in every radiological finding between the cirrhosis and control groups, p-values ranging from < 0.0001 to 0.03. The results are summarized in Figure 5.

In the cirrhosis group, the ratio between segment one and the right lobe was 0.8 (SD 0.3) and the modified ratio was 1.15 (SD 0.38). In the control group the respective values were 0.51 (SD 0.11). and 0.81 (SD 0.21). The difference in both S1/RL and S1/RLm values between the cirrhosis and control groups demonstrated very high statistical significance, with p-values of $p<0.0001$ and $p<0.0002$, respectively.

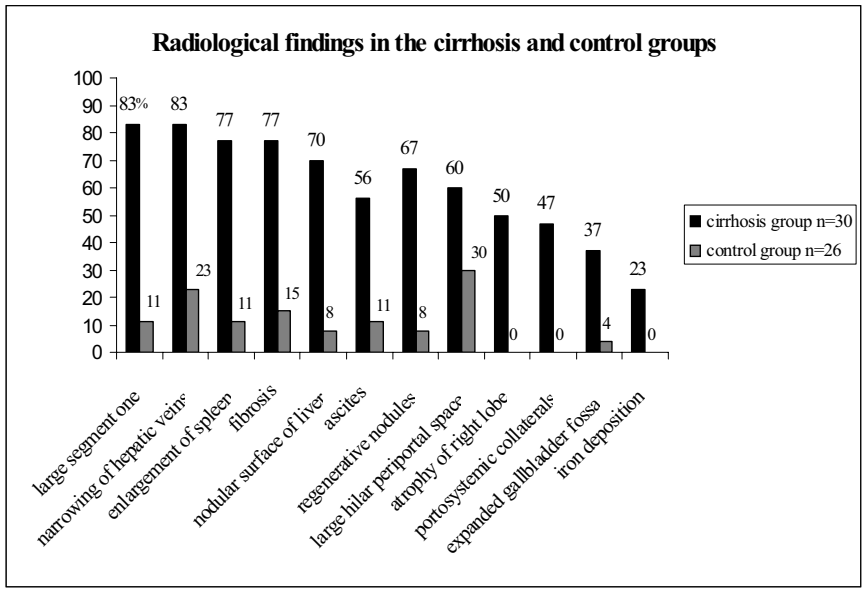
Radiological findings in the cirrhosis and control groups
100
90
80
70
60
50
40
30
20
10
0
83%
11
83
23
77
11
77
15
70
8
56
11
67
8
60
30
50
0
47
0
37
4
23
0
cirrhosis group n=30
control group n=26
large segment one
narrowing of hepatic vein
enlargement of spleen
fibrosis
nodular surface of liver
ascites
regenerative nodules
large hilar periportal space
atrophy of right lobe
portosystemic collaterals
expanded gallbladder fossa
iron deposition

Figure 5.

## *10. DISCUSSION*

### *10.1. Lesion detection with MRI, MDCT and IOUS*

The relative accuracy of CT compared with MRI has been the subject of numerous reports in the literature, with conflicting results (142, 143, 145, 157). Most studies are difficult to interpret with regard to currently available technology. What was true 5 years ago is not necessarily true today, in view of the significant advances made during recent years in MRI and especially in CT (MDCT). Few studies have compared what would be regarded as state-of-the-art MRI and CT techniques.

In the past, MRI was reported to surpass the performance of spiral helical CT in lesion detection (143). However, CT arterial portography (CTAP) was long regarded as the nonoperative gold standard for the imaging detection of hepatic lesions. Semelka et al. (142, 145) found MRI, including dynamic contrast-enhanced sequences, to be less sensitive than CTAP, but with fewer false positive results thanks to its better lesion characterization. They found MRI to have greater diagnostic accuracy, while being considerably less invasive and less expensive. Unenhanced T1- and T2-weighted sequences have proved to be useful in lesion detection. Dynamic gadolinium-enhanced MR imaging has not improved lesion detectability. The rate of false negative and false positive observations has been higher in gadolinium-enhanced images (57). The addition of liver-specific contrast agents has further improved MRI sensitivity for focal liver lesions. Ferumoxide-enhanced MR imaging has been shown to be effective in preoperative liver assessment (81, 126). However, this was not included in our clinical routine due several cases of side effects of iron particles.

Advances in MDCT have challenged the superiority of MRI in liver imaging. MDCT allows fast multiphasic liver scanning. Thin (1.25-2.5 mm) sections can be obtained routinely in single breath-hold scans (133). The results of study III suggest that MDCT is more sensitive in lesion detection than Gd-enhanced MRI. This contradictory result may have several explanations, basically concerned with the technical improvements introduced through MDCT. In the present investigation thin slices of 2.5 mm were acquired, whereas in earlier studies (10, 142, 143, 145, 180), 5-10 mm slice thicknesses were used. High scanning parameters with a tube voltage of 120-140 kV and a current of 300-380 mAs were used to avoid noise and to achieve the best possible image quality. Weg et al. (170) reported that the use of 2.5 mm thick sections resulted in an 18% better detection rate than when 5 mm thick slices were used. The injected contrast material (150 ml) had a high iodine concentration (370

mg I/ml). In previous reports, the administration of a high concentration of contrast material has improved the detection of both hypervascular liver tumors such as HCC and hypovascular lesions such as colorectal metastases as a result of the greater tumor-to-liver contrast (3, 58). Moreover, in this investigation, dynamic triphasic contrast-enhanced scanning was utilized with arterial phase imaging in both its early and late phases. This method has been reported to improve the depiction of hypervascular liver tumors and to reduce the rate of false positive findings (117). The obvious disadvantage of MDCT with thin slices is high radiation dose. But in selected cases, especially when curative treatment is considered (e.g. liver surgery), the dose of radiation can not be the limiting factor.

All patients in whom MRI missed liver lesions had a history of chemotherapy. Cytotoxic agents can considerably alter lesion appearance in MR images. Chemotherapy-treated lesions have been reported to show low signal intensity in both T2- and T1-weighted images with negligible enhancement after gadolinium administration. In superficial lesions, capsule retraction may be the only sign of metastases (13).

At present, intraoperative ultrasonography is regarded as the most accurate technique for liver tumor imaging. Several earlier reports have shown that IOUS is more sensitive in lesion detection than helical CT (44, 69, 81, 156, 167, 180). However, neither thin slices (2.5 mm), triphasic imaging nor high concentration contrast material were used in these studies. The results of the present study show that MDCT with thin slices and high volume, high concentration iodine contrast material is comparable with IOUS in lesion detection.

***10.2. Extrahepatic disease and vascular proximity***

According to the present results, IOUS with palpation performed better than MRI and MDCT in depicting extrahepatic disease. This may have several explanations. The MR imaging protocol used did not include a double dose of gadolinium, delayed imaging (5-10 minutes after injection), or coronal plane scanning. These methods are considered to be more effective than CT in the detection of malignant extrahepatic disease, especially involving the liver capsule and peritoneum (93, 95). Lymph nodes were detected with MRI in two patients and with MDCT in seven patients, but with both methods, however, only in one case were lymph nodes considered to be potentially malignant. The radiological criteria for lymph node malignancy are commonly considered to be the size (>1.5 cm) and spherical shape of lymph nodes. Moreover, it has been demonstrated that the macroscopic appearance of lymph nodes is unreliable in determining micrometastases (129). Routine lymph node palpation and

sampling are therefore mandatory to identify patients with extrahepatic extension of disease (49).

Vascular proximity was correctly assessed with the use of MDCT in 98% of lesions, compared with 87% for MRI**.** The difference was statistically significant (p=0.002). The difference may be partly due to the fact that MR images were obtained only in the transaxial plane, while MDCT images were also evaluated using a CT workstation, where multiplanar reformations could be reconstructed when necessary. In depicting the vascular proximity of lesions, MDCT was comparable with IOUS and resection histopathology, and no statistical significance (p=0.125) was observed. The results suggest that the preoperative assessment of vascular proximity is accurately determined using MDCT with multiplanar reformations.

### *10.3. Lesion characterization*

#### *10.3.1. Collection of sequences*

The results show that the classification into malignant and benign liver lesions, and the assessment of specific diagnosis were most reliably achieved when all sequences were collectively evaluated. Several previous investigations also advocate the use of a combination of sequences in liver diagnostics (28, 97, 123, 144). Coulam et al. (28) reported a sensitivity of 97% and a specificity of 95% in revealing clinically relevant focal liver lesions using a T1-weighted multiphase contrast-enhanced 3D sequence. However, they regarded unenhanced T1- and T2-weighted sequences as helpful in lesion characterization. This assumption is supported by previous reports of similar enhancement patterns for both benign and malignant liver lesions (97, 172, 179).

#### *10.3.2. Unenhanced and gadolinium-enhanced T1-weighted sequences*

According to the present results, the best individual sequence in distinguishing between malignant and benign liver lesions is the dynamic Gd-enhanced T1-weighted sequence. This sequence also demonstrated the highest success in the assessment of specific diagnosis, with a 63% rate of correct diagnosis. Several previous studies support this result as Gd-enhancement, particularly when used in a dynamic fashion in different phases of enhancement, has been considered to be highly important in liver tumor characterization (28, 46, 56, 125, 147, 148, 172).

As shown by the results of this study and by earlier investigations, the unenhanced T1-weighted sequence is of limited value in lesion characterization (28, 56, 176). Only 62% of

lesions were correctly classified and specific diagnosis was assessed in 46% of cases. The T1-weighted sequence is, however, useful for the evaluation of hemorrhagic lesions, tumors with a high fat or copper content such as hepatocellular carcinoma and hepatic adenoma, and lesions that contain melanin such as melanoma metastases. All these lesions may demonstrate a high signal intensity in unenhanced T1-weighted images (77). The current results support these previous findings. HCCs were correctly diagnosed in 76% of cases. This compares well with the result gained in the study conducted by Pauleit et al. (121) with correct characterization of HCC using an unenhanced T1-weighted sequence in 71% of cases. Although the benefit of the unenhanced T1-weighted sequence is considered to be in lesion detection (57), it is also valuable in lesion characterization.

#### *10.3.3. T2-weighted sequences*

T2-weighted sequences are discussed in chapter 8.4., Characterization of hemangiomas by MRI.

### *10.4. Characterization of hemangiomas by MRI*

The main value of T2-weighted MR imaging is in the diagnosis of hemangiomas. T2-weighted MRI has limited value in the characterization of malignant liver lesions because of the wide variety of lesion appearances (146, 159). Reduced lesion conspicuity and the overlap in signal intensity characteristic of benign and malignant nodules diminished the diagnostic value of T2-weighted images in cases of cirrhotic liver, too (64).

The results of study I demonstrate that additional lesion information is obtained with the true FISP and T2-weighted sequences, especially in hemangioma diagnostics. Hepatic hemangiomas were correctly diagnosed with great confidence and without Gd enhancement. The true FISP sequence and HASTE correctly gave the specific diagnosis in 92% (mean value) and in 84% (mean value) of hemangioma cases, respectively. All hemangiomas appeared bright in true FISP images, while the malignant liver foci were nearly isointense relative to normal liver parenchyma. The high signal of hemangiomas is probably due to the fact that in the true FISP sequence, the FISP and PSIF (reverse FISP) echoes are produced at the same time, and thus only one combined signal is received. FISP produces images with T2*/T1 contrast due to the preserved transverse magnetization component, and PSIF produces images with heavy T2-weighting due to the very long echo times. Malignant liver lesions demonstrated nearly the same signal intensity compared to the surrounding normal liver

parenchyma in true FISP images. A similar finding has been reported with HASTE (162). Analysis of lesion CNR values supported the film reading. All hemangiomas demonstrated very high CNR values, while the CNRs for the malignant liver lesions were considerably lower. The difference in CNR values between hemangiomas and malignant liver lesions was highly statistically significant ($p<0.0001$).

The results indicate that both true FISP and HASTE are valuable tools in routine liver MRI protocol for distinguishing hepatic hemangiomas from liver malignancies, as previously suggested by Herborn et al. (62).

The specific diagnosis of hemangiomas was reached with Gd enhancement in 80% of cases. Hemangiomas may show various enhancement patterns (140, 172). Small hemangiomas, in particular, may demonstrate strong and uniform early arterial enhancement identical to that shown by hypervascular liver metastases and hepatocellular carcinoma (140). Hence, small liver lesions constitute a problem with Gd-enhanced MRI (97, 147, 172).

The results of study I indicate that small hemangiomas and malignant liver lesions can also be reliably differentiated from each other with the true FISP sequence. In the present study, of the 27 hemangiomas with a diameter of 1-2 cm, 25 and 23, respectively, were correctly diagnosed by the two readers. True FISP was superior to dynamic Gd-enhanced MRI in the characterization of small hepatic hemangiomas.

### *10.5. Liver cirrhosis*

According to the results of study IV, liver cirrhosis can be diagnosed with great confidence with MRI: the sensitivity was 87% (26/30) and the specificity 92%. Every Child-Pugh class B and C cirrhosis was correctly diagnosed. All four false negative cases were in Child-Pugh class A. Class A cirrhosis is often asymptomatic and may be discovered during a routine clinical examination or by biochemical screening. Morphologic changes of the liver are also seen less frequently in class A patients, especially in early cases (68).

The results indicate that the most characteristic MRI feature of liver cirrhosis is the enlargement of segment one. The cause of segment one hypertrophy is unclear, but it is thought to be linked to alterations in portal blood flow. Segmental hepatic blood volume is related to portal venous blood, which carries various trophic factors (160). The blood supply

to segment one arises predominantly from the left branches or from bifurcation of the portal vein (113). However, a branch to the caudate process from the posterior segmental branch is present in 51% of cases (112). The segment one branches have a shorter intrahepatic course than other vessels, and this may be a factor in the relatively greater preservation of segment one blood supply (32). Atrophy of the right lobe is also considered to be related to changes in portal blood supply (4). Atrophy of the right lobe was observed in 50% of our cirrhotic cases.

The ratio between the transverse diameters of segment one and right lobe has previously been measured using the main portal vein bifurcation as a landmark to divide the lobes. A ratio greater than 0.65 has been considered to be sensitive and specific for cirrhosis (59). Recently, however, it has been reported that the bifurcation of the right portal vein is even more sensitive and specific for representing the division between segment one and the right lobe (4). According to the present results, however, both measurements were equally accurate in diagnosing cirrhosis.

A new observation in study IV was that, in cirrhotic livers, the hepatic veins and vena cava were narrowed. This feature was present in 83% of the patients. Hepatic fibrosis causes attenuation of the intrahepatic portal and hepatic venous branches, and the hepatic vascular bed is reduced. Impaired drainage of blood from the liver, caused by compression of hepatic venous tributaries by regenerative nodules and fibrosis, increases the resistance to portal flow (124).

In this study, parenchymal fibrosis was also a frequent imaging feature (77% of patients). Fibrosis appeared as regions of low signal intensity in unenhanced T1-weighted images. Fibrosis usually showed mild enhancement in MR images and was seen with high intensity in T2-weighted images. Fibrosis is usually diffuse, but a patchy focal appearance is also possible mimicking hepatocellular carcinoma on imaging (31).

As the fibrosis progresses, hepatic failure and portal hypertension ensue. Portal hypertension results from obstruction of hepatic sinusoids. Signs of portal hypertension, such as enlargement of the spleen, venous collaterals and ascites, were commonly observed in the present study. During the early stages of portal hypertension, the portal system dilates but flow is maintained. Later, numerous portosystemic collateral pathways from the high-pressure portal system to the low-pressure systemic circulation develop, reducing the volume of flow to the liver and decreasing the size of the portal vein (68).

In the current study, 70% of the livers represented a nodular margin in patients with cirrhosis. This finding correlates directly with the size of underlying regenerative nodules. A surface that is smooth or deformed by multiple small nodules is typical in micronodular cirrhosis; a coarse nodularity of the margin is the result of macronodular cirrhosis (31). In the study by Di Lelio (30) nodular liver surface was seen in 88% of cirrhotic patients.

Cirrhosis may cause hepatic parenchymal iron deposition. In the cases studied here, however, this feature was present in only 23% of cirrhotic livers. The amount of iron in a cirrhotic liver can also vary depending on the etiology of the cirrhosis (107). The etiology of the cirrhosis in the present study was predominantly primary biliary cirrhosis, and iron was seen as low-signal siderotic nodules in T2-weighted images. Diffuse hepatic iron deposition is also possible in cirrhotic hepatic parenchyma, and with extensive fibrosis parenchyma can appear rather heterogeneous in T2-weighted images (65).

An expanded gall bladder fossa is considered to be a specific indicator of cirrhosis (66). In the present study material this finding appeared in conjunction with 37% of cirrhotic livers. Moreover, there was only one false positive case. The results thus agree with the earlier findings that an expanded gall bladder fossa, although not a common finding, is highly specific to liver cirrhosis. Enlargement of the hilar periportal space, seen in 60% of the cases in this study, is also caused by morphologic changes in the liver (67). This sign was also seen in 30% of the livers in the control group, and is considered to be the earliest sign of incipient cirrhosis.

Liver cirrhosis is associated with a markedly increased risk of hepatocellular carcinoma, and cirrhosis has been reported to be present in 90% of patients with HCC (169). In the present study, 30% of patients demonstrated HCC. One false positive case was also noted. This was a large regenerative nodule. In previous studies, MRI has proved to be highly sensitive in depicting HCC (35). However, one-third of suspected tumors may be false positive lesions (6) due to fact that signal intensities and enhancement patterns overlap between small HCCs and degenerative and especially dysplastic nodules (64, 70).

### *10.6. Future aspects of liver MRI*

Liver MRI has been and still is the subject of great interest. Yet it is impossible to predict which of today's topics in radiological literature have true value in future clinical work.

The relative values of MDCT and MRI in liver imaging have not been established, since at the moment there are only a few comparative studies available on MDCT and MRI in liver diagnostics. MDCT has obvious advantages over MRI. Technical advances in hardware and software mean that MDCT allows high-quality multiplanar reformations and three-dimensional models from raw data. 3D models constructed from MDCT raw data are already being used in the preoperative evaluation of living donor liver transplantation and these models probably will play important role in planning of tumor resection (37, 52, 75).

There continues to be much interest in several tissue-specific contrast agents (11, 81). Despite the broad spectrum of investigation, none of these contrast agents has yet made a true breakthrough in clinical work. Tumor-targeted MR contrast agents may play an important role in the future (128). Preliminary studies have been made of the 3 T field strength in the liver (29), but there are many technical problems to solve, especially concerning artifacts. MR cholangiopancreatography will probably maintain its position as an excellent tool for non-invasive evaluation of the bile ducts (91). MRI perfusion imaging has shown promising results in determining the severity of cirrhosis and portal hypertension (2).

Although methods such as PET and CT PET with potential applications in liver diagnostics are evolving, MRI will certainly continue to play an important role in liver imaging because of its superior soft tissue contrast compared to any other imaging modality.

## *11. CONCLUSIONS*

1. Triphasic MDCT with thin slices and high-volume, high-concentration contrast material is a very sensitive and noninvasive technique in preoperative liver assessment. Both lesion detection and the depiction of lesion in relation to vascular structures were more precise with MDCT than with MRI. However, both methods had only a limited value in the detection of extrahepatic disease.

2. The use of multiple sequences in conjunction with Gd enhancement makes MRI extremely useful in liver lesion classification, although its potential in the assessment of specific diagnosis is only moderate.

3. The true FISP sequence has potential in the diagnosis of hemangiomas and can differentiate reliably between hemangiomas and malignant liver lesions.

4. MRI is an accurate method for diagnosing Child B and C cirrhosis. The most characteristic imaging features of cirrhosis were a large segment one, narrowing of the hepatic veins and signs of portal hypertension, fibrosis and a nodular margin of the liver. MRI is also a sensitive way to detect occult hepatocellular carcinoma.

## *12. ACKNOWLEDGEMENTS*

This study was carried out at the Medical Imaging Center and at the Transplantation and Liver Surgery Clinic, Helsinki University Hospital.

I wish to express my deep gratitude to my supervisor Professor Krister Höckerstedt, M.D., for his interest in my work and for his constant personal encouragement. I appreciate his diplomatic way of supervising: he always gave help at the right time and in the right way.
I am greatly indebted to Docent Pekka Tervahartiala, M.D., my other supervisor and current chief, for his great patience. His perfectionism certainly improved the manuscripts and taught me a lot. I am grateful to Docent Juha Halavaara, M.D., whose verbal brilliance was a tremendous help. Despite their heavy commitments, Pekka and Juha always found time to read my text and also showed continual support and tireless interest in this study. Their enthusiasm has encouraged me immensely. I am grateful to Docent Helena Isoniemi, M.D., the initiator of this study, for her constant guidance and valuable advice. I greatly admire Helena's stamina: despite having worked throughout the night Helena still had the energy to help me. Her advice was always practical and easy to accept.

My warm thanks go to Docent Heikki Mäkisalo, M.D., for participating in this study and for his encouragement and support. I also owe thanks to Docent Leena Halme, M.D., who gave me much useful advice and showed great interest in my work. Heikki, Leena, Helena, Krisse and the rest of the transplantation team have provided strong support in my clinical work. It has been inspiring to work with them. Furthermore I express them thanks for their feedback and for teaching me clinical aspects of transplantations and hepatology. These are, as a matter of fact, essential to becoming a better radiologist.

I wish to thank Docent Eija Pääkkö, M.D., and Docent Tapani Tikkakoski, M.D., for their expert advice during revisions of the manuscript.

My sincere thanks go to Professor Leena Laasonen, M.D., my former chief, for her continual support and tireless interest. I thank Professor Leena Kivisaari, M.D., for her constructive criticism. I owe my deepest gratitude to Professor Hannu Suoranta, M.D., who made such pertinent comments about my manuscript.

I wish to thank to my cousin Jussi Numminen, M.D., for helping me with the statistics and Maarit Palomäki, M.D., for participating in this study.

I want to say a very special thank-you to Paavo Kettunen, M.D., and Ilmari Anttinen, M.D., two wonderful personalities and radiologists, who have been the best teachers in radiology I ever had.

I sincerely thank radiographer Pentti Pölönen and Helena Lustig for arranging the study data.

I wish to thank my colleagues Marina Rosliakova, M.D., Esko Tierala, M.D., Pertti Paukku, M.D. and Anni Suomalainen, D.D.S. at the Department of Radiology at the Surgical Hospital for their help and optimistic attitude over these years.

The language revision was carried out by Philip Mason, B.Sc.

The help of my sisters Leena and Taru has meant a lot of me. Leena always found time to listen to my troubles, while Taru was an immense help with my numerous computer problems and also helped me with the huge job of organizing the data. Thanks to my nieces and nephews Linda, Laura, Joel, Sara, Jussi for being there and for keeping my spirits up and as well for all the time we have spent together.

Finally, I would like to thank my mother and late father for teaching me the basic principles of life: in real life many tasks can be hard, time consuming and frustrating. Nevertheless you still have to do them as well as you can. Always finish what you have started.

This study was financially supported by the Radiological Society of Finland and Pehr Oscar Klingendahl Foundation.

Helsinki, October 2004

Kirsti Numminen

## *13. REFERENCES*


1. Abbitt PL. Ultrasonography. Update on liver technique. Radiol Clin North Am 36:299-307, 1998.

2. Annet L, Materne R, Danse E, Jamart J, Horsmans Y, Van Beers BE. Hepatic flow parameters measured with MR imaging and Doppler US: correlations with degree of cirrhosis and portal hypertension. Radiology 229:409-414, 2003.

3. Awai K, Takada K, Onishi H, Hori S. Aortic and hepatic enhancement and tumor-to-liver contrast: analysis of the effect of different concentrations of contrast material at multi-detector row helical CT. Radiology 224:757-763, 2002.

4. Awaya H, Mitchell DG, Kamishima T, Holland G, Ito K, Matsumoto T. Cirrhosis: modified caudate-right lobe ratio. Radiology 224:769-774, 2002.

5. Baker ME, Pelley R. Hepatic metastases: basic principles and implications for radiologists. Radiology 197:329-337, 1995.

6. Baron RL, Peterson MS. From the RSNA refresher courses: screening the cirrhotic liver for hepatocellular carcinoma with CT and MR imaging: opportunities and pitfalls. Radiographics 21:117-132, 2001.

7. Bartolozzi C, Lencioni R, Donati F, Cioni D. Abdominal MR: liver and pancreas. Eur Radiol 9:1496-1512, 1999.

8. Beavers KL, Semelka RC. MRI evaluation of the liver. Semin Liver Dis 21:161-177, 2001.

9. Bjoro K, Friman S, Hockerstedt K, et al. Liver transplantation in the Nordic countries, 1982-1998: changes of indications and improving results. Scand J Gastroenterol 34:714-722, 1999.

10. Bloed W, van Leeuwen MS, Borel Rinkes IH. Role of intraoperative ultrasound of the liver with improved preoperative hepatic imaging. Eur J Surg 166:691-695, 2000.

11. Bluemke DA, Weber TM, Rubin D, et al. Hepatic MR imaging with ferumoxides: multicenter study of safety and effectiveness of direct injection protocol. Radiology 228:457-464, 2003.

12. Boberg KM, Aadland E, Jahnsen J, Raknerud N, Stiris M, Bell H. Incidence and prevalence of primary biliary cirrhosis, primary sclerosing cholangitis, and

autoimmune hepatitis in a Norwegian population. Scand J Gastroenterol 33:99-103, 1998.

13. Braga L, Semelka RC, Pedro MS, de Barros N. Post-treatment malignant liver lesions. MR imaging. Magn Reson Imaging Clin N Am 10:53-73, 2002.

14. Braun AH, Achterrath W, Wilke H, Vanhoefer U, Harstrick A, Preusser P. New systemic frontline treatment for metastatic colorectal carcinoma. Cancer 100:1558-1577, 2004.

15. Brenner DA, Alcorn JM. Pathogenesis of hepatic fibrosis. In: Kaplowitz N, ed. Liver and biliary disease. Baltimore: Williams&Williams, 1992.

16. Brown JJ, Naylor MJ, Yagan N. Imaging of hepatic cirrhosis. Radiology 202:1-16, 1997.

17. Cady B, Jenkins RL, Steele GD, Jr., et al. Surgical margin in hepatic resection for colorectal metastasis: a critical and improvable determinant of outcome. Ann Surg 227:566-571, 1998.

18. Campeau NG, Johnson CD, Felmlee JP, et al. MR imaging of the abdomen with a phased-array multicoil: prospective clinical evaluation. Radiology 195:769-776, 1995.

19. Carr DH, Brown J, Bydder GM, et al. Gadolinium-DTPA as a contrast agent in MRI: initial clinical experience in 20 patients. AJR Am J Roentgenol 143:215-224, 1984.

20. Catasca JV, Mirowitz SA. T2-weighted MR imaging of the abdomen: fast spin-echo vs conventional spin-echo sequences. AJR Am J Roentgenol 162:61-67, 1994.

21. Caudana R, Morana G, Pirovano GP, et al. Focal malignant hepatic lesions: MR imaging enhanced with gadolinium benzyloxypropionictetra-acetate (BOPTA)--preliminary results of phase II clinical application. Radiology 199:513-520, 1996.

22. Chen MF, Tsai HP, Jeng LB, et al. Prognostic factors after resection for hepatocellular carcinoma in noncirrhotic livers: univariate and multivariate analysis. World J Surg 27:443-447, 2003.

23. Choi H, Loyer EM, DuBrow RA, et al. Radio-frequency ablation of liver tumors: assessment of therapeutic response and complications. Radiographics 21:41-54, 2001.

24. Choti MA, Sitzmann JV, Tiburi MF, et al. Trends in long-term survival following liver resection for hepatic colorectal metastases. Ann Surg 235:759-766, 2002.

25. Chung KY, Mayo-Smith WW, Saini S, Rahmouni A, Golli M, Mathieu D. Hepatocellular adenoma: MR imaging features with pathologic correlation. AJR Am J Roentgenol 165:303-308, 1995.

26. Corrao G, Ferrari P, Zambon A, Torchio P, Arico S, Decarli A. Trends of liver cirrhosis mortality in Europe, 1970-1989: age-period-cohort analysis and changing alcohol consumption. Int J Epidemiol 26:100-109, 1997.

27. Couinaud C. Le Foie. In: Couinaud C, ed. Etudes anatomiques et chirurgicales. Paris: Masson, 1957.

28. Coulam CH, Chan FP, Li KC. Can a multiphasic contrast-enhanced three-dimensional fast spoiled gradient-recalled echo sequence be sufficient for liver MR imaging? AJR Am J Roentgenol 178:335-341, 2002.

29. de Bazelaire CM, Duhamel GD, Rofsky NM, Alsop DC. MR imaging relaxation times of abdominal and pelvic tissues measured in vivo at 3.0 T: preliminary results. Radiology 230:652-659, 2004.

30. Di Lelio A, Cestari C, Lomazzi A, Beretta L. Cirrhosis: diagnosis with sonographic study of the liver surface. Radiology 172:389-392, 1989.

31. Dodd GD, 3rd, Baron RL, Oliver JH, 3rd, Federle MP. Spectrum of imaging findings of the liver in end-stage cirrhosis: part I, gross morphology and diffuse abnormalities. AJR Am J Roentgenol 173:1031-1036, 1999.

32. Doehner GA. The portal venous system: its pathological roentgen anatomy. Radiology 64:675-689, 1955.

33. Drane WE. Scintigraphic techniques for hepatic imaging. Update for 2000. Radiol Clin North Am 36:309-318, 1998.

34. Duerk JL, Lewin JS, Wendt M, Petersilge C. Remember true FISP? A high SNR, near 1-second imaging method for T2-like contrast in interventional MRI at .2 T. J Magn Reson Imaging 8:203-208, 1998.

35. Earls JP, Theise ND, Weinreb JC, et al. Dysplastic nodules and hepatocellular carcinoma: thin-section MR imaging of explanted cirrhotic livers with pathologic correlation. Radiology 201:207-214, 1996.

36. Earls JP, Rofsky NM, DeCorato DR, Krinsky GA, Weinreb JC. Echo-train STIR MRI of the liver: comparison of breath-hold and non-breath-hold imaging strategies. J Magn Reson Imaging 9:87-92, 1999.

37. Erbay N, Raptopoulos V, Pomfret EA, Kamel IR, Kruskal JB. Living donor liver transplantation in adults: vascular variants important in surgical planning for donors and recipients. AJR Am J Roentgenol 181:109-114, 2003.

38. Fernandez MP, Redvanly RD. Primary hepatic malignant neoplasms. Radiol Clin North Am 36:333-348, 1998.

39. Foley WD, Kneeland JB, Cates JD, et al. Contrast optimization for the detection of focal hepatic lesions by MR imaging at 1.5 T. AJR Am J Roentgenol 149:1155-1160, 1987.

40. Foley WD, Mallisee TA, Hohenwalter MD, Wilson CR, Quiroz FA, Taylor AJ. Multiphase hepatic CT with a multirow detector CT scanner. AJR Am J Roentgenol 175:679-685, 2000.

41. Foley WD. Special focus session: multidetector CT: abdominal visceral imaging. Radiographics 22:701-719, 2002.

42. Fong Y, Cohen AM, Fortner JG, et al. Liver resection for colorectal metastases. J Clin Oncol 15:938-946, 1997.

43. Fong Y, Fortner J, Sun RL, Brennan MF, Blumgart LH. Clinical score for predicting recurrence after hepatic resection for metastatic colorectal cancer: analysis of 1001 consecutive cases. Ann Surg 230:309-318, 1999.

44. Fortunato L, Clair M, Hoffman J, et al. Is CT portography (CTAP) really useful in patients with liver tumors who undergo intraoperative ultrasonography (IOUS)? Am Surg 61:560-565, 1995.

45. Frahm J, Haase A, Matthaei D. Rapid NMR imaging of dynamic processes using the FLASH technique. Magn Reson Med 3:321-327, 1986.

46. Fujita T, Ito K, Honjo K, Okazaki H, Matsumoto T, Matsunaga N. Detection of hepatocellular carcinoma: comparison of T2-weighted breath-hold fast spin-echo sequences and high-resolution dynamic MR imaging with a phased-array body coil. J Magn Reson Imaging 9:274-279, 1999.

47. Gaa J, Hatabu H, Jenkins RL, Finn JP, Edelman RR. Liver masses: replacement of conventional T2-weighted spin-echo MR imaging with breath-hold MR imaging. Radiology 200:459-464, 1996.

48. Gazelle GS, Goldberg SN, Solbiati L, Livraghi T. Tumor ablation with radio-frequency energy. Radiology 217:633-646, 2000.

49. Gibbs JF, Weber TK, Rodriguez-Bigas MA, Driscoll DL, Petrelli NJ. Intraoperative determinants of unresectability for patients with colorectal hepatic metastases. Cancer 82:1244-1249, 1998.

50. Gordon SC, Reddy KR, Livingstone AS, Jeffers LJ, Schiff ER. Resolution of a contraceptive-steroid-induced hepatic adenoma with subsequent evolution into hepatocellular carcinoma. Ann Intern Med 105:547-549, 1986.

51. Graig GR, Peters RL, Edmonson HA. Tumors of the liver and intrahepatic bile ducts. In:Atlas of tumor pathology. Washington: Armed Forces Institute of Pathology, 1989.

52. Guiney MJ, Kruskal JB, Sosna J, Hanto DW, Goldberg SN, Raptopoulos V. Multi-detector row CT of relevant vascular anatomy of the surgical plane in split-liver transplantation. Radiology 229:401-407, 2003.

53. Halavaara JT, Lamminen AE, Bondestam S, Standertskjold-Nordenstam CG, Hamberg LM. Detection of focal liver lesions with superparamagnetic iron oxide: value of STIR and SE imaging. J Comput Assist Tomogr 18:897-904, 1994.

54. Halavaara JT, Lamminen AE. MnDPDP as a negative hepatic contrast agent: evaluation of STIR imaging compared with T1-weighted SE and GE techniques. J Comput Assist Tomogr 21:94-99, 1997.

55. Hamm B, Vogl TJ, Branding G, et al. Focal liver lesions: MR imaging with Mn-DPDP--initial clinical results in 40 patients. Radiology 182:167-174, 1992.

56. Hamm B, Thoeni RF, Gould RG, et al. Focal liver lesions: characterization with nonenhanced and dynamic contrast material-enhanced MR imaging. Radiology 190:417-423, 1994.

57. Hamm B, Mahfouz AE, Taupitz M, et al. Liver metastases: improved detection with dynamic gadolinium-enhanced MR imaging? Radiology 202:677-682, 1997.

58. Hanninen EL, Vogl TJ, Felfe R, et al. Detection of focal liver lesions at biphasic spiral CT: randomized double-blind study of the effect of iodine concentration in contrast materials. Radiology 216:403-409, 2000.

59. Harbin WP, Robert NJ, Ferrucci JT, Jr. Diagnosis of cirrhosis based on regional changes in hepatic morphology: a radiological and pathological analysis. Radiology 135:273-283, 1980.

60. Henderson MJ, Vogt D. Non-transplant surgery and the liver. In: 0´Grady JG, Lake JR, Howdle PD, ed. Comprehensive clinical hepatology. London: Mosby, 2000.

61. Hennig J, Nauerth A, Friedburg H. RARE imaging: a fast imaging method for clinical MR. Magn Reson Med 3:823-833, 1986.

62. Herborn CU, Vogt F, Lauenstein TC, Goyen M, Debatin JF, Ruehm SG. MRI of the liver: can True FISP replace HASTE? J Magn Reson Imaging 17:190-196, 2003.

63. Hittmair K, Trattnig S, Herold CJ, Breitenseher M, Kramer J. Comparison between conventional and fast spin-echo stir sequences. Acta Radiol 37:943-949, 1996.

64. Hussain HK, Syed I, Nghiem HV, et al. T2-weighted MR imaging in the assessment of cirrhotic liver. Radiology 230:637-644, 2004.

65. Ito K, Mitchell DG, Gabata T, et al. Hepatocellular carcinoma: association with increased iron deposition in the cirrhotic liver at MR imaging. Radiology 212:235-240, 1999.

66. Ito K, Mitchell DG, Gabata T, Hussain SM. Expanded gallbladder fossa: simple MR imaging sign of cirrhosis. Radiology 211:723-726, 1999.

67. Ito K, Mitchell DG, Gabata T. Enlargement of hilar periportal space: a sign of early cirrhosis at MR imaging. J Magn Reson Imaging 11:136-140, 2000.

68. Ito K, Mitchell DG, Siegelman ES. Cirrhosis: MR imaging features. Magn Reson Imaging Clin N Am 10:75-92, vi, 2002.

69. Jarnagin WR, Bach AM, Winston CB, et al. What is the yield of intraoperative ultrasonography during partial hepatectomy for malignant disease? J Am Coll Surg 192:577-583, 2001.

70. Jeong YY, Mitchell DG, Kamishima T. Small (<20 mm) enhancing hepatic nodules seen on arterial phase MR imaging of the cirrhotic liver: clinical implications. AJR Am J Roentgenol 178:1327-1334, 2002.

71. Johnson P. Malignant tumors of the liver. In: O´Grady JG, Lake JR, Howdle PD, ed. Comprehensive clinical hepatology. London: Mosby, 2000.

72. Kabbinavar F, Hurwitz HI, Fehrenbacher L, et al. Phase II, randomized trial comparing bevacizumab plus fluorouracil (FU)/leucovorin (LV) with FU/LV alone in patients with metastatic colorectal cancer. J Clin Oncol 21:60-65, 2003.

73. Kadoya M, Matsui O, Nakanuma Y, et al. Ciliated hepatic foregut cyst: radiologic features. Radiology 175:475-477, 1990.

74. Kadoya M, Matsui O, Takashima T, Nonomura A. Hepatocellular carcinoma: correlation of MR imaging and histopathologic findings. Radiology 183:819-825, 1992.

75. Kanazawa A, Hirohashi K, Tanaka H, et al. Usefulness of three-dimensional computed tomography in a living-donor extended right lobe liver transplantation. Liver Transpl 8:1076-1079, 2002.

76. Karhunen PJ. Benign hepatic tumours and tumour like conditions in men. J Clin Pathol 39:183-188, 1986.

77. Kelekis NL, Semelka RC, Woosley JT. Malignant lesions of the liver with high signal intensity on T1-weighted MR images. J Magn Reson Imaging 6:291-294, 1996.

78. Kemmerer SR, Mortele KJ, Ros PR. CT scan of the liver. Radiol Clin North Am 36:247-261, 1998.

79. Keogan MT, Edelman RR. Technologic advances in abdominal MR imaging. Radiology 220:310-320, 2001.

80. Kerlin P, Davis GL, McGill DB, Weiland LH, Adson MA, Sheedy PF, 2nd. Hepatic adenoma and focal nodular hyperplasia: clinical, pathologic, and radiologic features. Gastroenterology 84:994-1002, 1983.

81. Kim SK, Kim SH, Lee WJ, et al. Preoperative detection of hepatocellular carcinoma: ferumoxides-enhanced versus mangafodipir trisodium-enhanced MR imaging. AJR Am J Roentgenol 179:741-750, 2002.

82. Kinkel K, Lu Y, Both M, Warren RS, Thoeni RF. Detection of hepatic metastases from cancers of the gastrointestinal tract by using noninvasive imaging methods (US, CT, MR imaging, PET): a meta-analysis. Radiology 224:748-756, 2002.

83. Kopp AF, Heuschmid M, Claussen CD. Multidetector helical CT of the liver for tumor detection and characterization. Eur Radiol 12:745-752, 2002.

84. Krinsky GA, Lee VS. MR imaging of cirrhotic nodules. Abdom Imaging 25:471-482, 2000.

85. Laing AD, Gibson RN. MRI of the liver. J Magn Reson Imaging 8:337-345, 1998.

86. Lang BH, Poon RT, Fan ST, Wong J. Perioperative and long-term outcome of major hepatic resection for small solitary hepatocellular carcinoma in patients with cirrhosis. Arch Surg 138:1207-1213, 2003.

87. Larson RE, Semelka RC, Bagley AS, Molina PL, Brown ED, Lee JK. Hypervascular malignant liver lesions: comparison of various MR imaging pulse sequences and dynamic CT. Radiology 192:393-399, 1994.

88. Lee MJ, Hahn PF, Saini S, Mueller PR. Differential diagnosis of hyperintense liver lesions on T1-weighted MR images. AJR Am J Roentgenol 159:1017-1020, 1992.

89. Lee VS, Lavelle MT, Rofsky NM, et al. Hepatic MR imaging with a dynamic contrast-enhanced isotropic volumetric interpolated breath-hold examination: feasibility, reproducibility, and technical quality. Radiology 215:365-372, 2000.

90. Lewis KH, Chezmar JL. Hepatic metastases. Magn Reson Imaging Clin N Am 5:319-330, 1997.

91. Limanond P, Raman SS, Ghobrial RM, Busuttil RW, Lu DS. The utility of MRCP in preoperative mapping of biliary anatomy in adult-to-adult living related liver transplant donors. J Magn Reson Imaging 19:209-215, 2004.

92. Llovet JM, Burroughs A, Bruix J. Hepatocellular carcinoma. Lancet 362:1907-1917, 2003.

93. Low RN, Semelka RC, Worawattanakul S, Alzate GD, Sigeti JS. Extrahepatic abdominal imaging in patients with malignancy: comparison of MR imaging and helical CT, with subsequent surgical correlation. Radiology 210:625-632, 1999.

94. Low RN. MR imaging of the liver using gadolinium chelates. Magn Reson Imaging Clin N Am 9:717-743, vi, 2001.

95. Low RN. Gadolinium-enhanced MR imaging of liver capsule and peritoneum. Magn Reson Imaging Clin N Am 9:803-819, vii, 2001.

96. Lu DS, Saini S, Hahn PF, et al. T2-weighted MR imaging of the upper part of the abdomen: should fat suppression be used routinely? AJR Am J Roentgenol 162:1095-1100, 1994.

97. Mahfouz AE, Hamm B, Taupitz M, Wolf KJ. Hypervascular liver lesions: differentiation of focal nodular hyperplasia from malignant tumors with dynamic gadolinium-enhanced MR imaging. Radiology 186:133-138, 1993.

98. Mahfouz AE, Hamm B, Wolf KJ. Peripheral washout: a sign of malignancy on dynamic gadolinium-enhanced MR images of focal liver lesions. Radiology 190:49-52, 1994.

99. Mansfield P, Pykett IL, Morris PG. Human whole body line-scan imaging by NMR. Br J Radiol 51:921-922, 1978.

100. Martin J, Sentis M, Puig J, et al. Comparison of in-phase and opposed-phase GRE and conventional SE MR pulse sequences in T1-weighted imaging of liver lesions. J Comput Assist Tomogr 20:890-897, 1996.

101. Mathiesen UL, Ekermo B, Foberg U, et al. Anti-hepatitis C virus screening will reduce the incidence of post-transfusion hepatitis C also in low-risk areas. Scand J Gastroenterol 27:443-448, 1992.

102. Matsui O, Kadoya M, Kameyama T, et al. Adenomatous hyperplastic nodules in the cirrhotic liver: differentiation from hepatocellular carcinoma with MR imaging. Radiology 173:123-126, 1989.

103. Mattison GR, Glazer GM, Quint LE, Francis IR, Bree RL, Ensminger WD. MR imaging of hepatic focal nodular hyperplasia: characterization and distinction from primary malignant hepatic tumors. AJR Am J Roentgenol 148:711-715, 1987.

104. McFarland EG, Mayo-Smith WW, Saini S, Hahn PF, Goldberg MA, Lee MJ. Hepatic hemangiomas and malignant tumors: improved differentiation with heavily T2-weighted conventional spin-echo MR imaging. Radiology 193:43-47, 1994.

105. McGhana JP, Dodd GD, 3rd. Radiofrequency ablation of the liver: current status. AJR Am J Roentgenol 176:3-16, 2001.

106. Meissner K. Hemorrhage caused by ruptured liver cell adenoma following long-term oral contraceptives: a case report. Hepatogastroenterology 45:224-225, 1998.

107. Mergo PJ, Ros PR, Buetow PC, Buck JL. Diffuse disease of the liver: radiologic-pathologic correlation. Radiographics 14:1291-1307, 1994.

108. Mergo PJ, Ros PR. Benign lesions of the liver. Radiol Clin North Am 36:319-331, 1998.

109. Mitchell DG, Saini S, Weinreb J, et al. Hepatic metastases and cavernous hemangiomas: distinction with standard- and triple-dose gadoteridol-enhanced MR imaging. Radiology 193:49-57, 1994.

110. Mitsudo K, Watanabe Y, Saga T, et al. Nonenhanced hepatic cavernous hemangioma with multiple calcifications: CT and pathologic correlation. Abdom Imaging 20:459-461, 1995.

111. Miyazaki T, Yamashita Y, Tsuchigame T, Yamamoto H, Urata J, Takahashi M. MR cholangiopancreatography using HASTE (half-Fourier acquisition single-shot turbo spin-echo) sequences. AJR Am J Roentgenol 166:1297-1303, 1996.

112. Mizumoto R, Kawarada Y, Suzuki H. Surgical treatment of hilar carcinoma of the bile duct. Surg Gynecol Obstet 162:153-158, 1986.

113. Mizumoto R, Suzuki H. Surgical anatomy of the hepatic hilum with special reference to the caudate lobe. World J Surg 12:2-10, 1988.

114. Morrin MM, Rofsky NM. Techniques for liver MR imaging. Magn Reson Imaging Clin N Am 9:675-696, v, 2001.

115. Motohara T, Semelka RC, Nagase L. MR imaging of benign hepatic tumors. Magn Reson Imaging Clin N Am 10:1-14, 2002.

116. Murakami T, Nakamura H, Tsuda K, et al. Contrast-enhanced MR imaging of intrahepatic cholangiocarcinoma: pathologic correlation study. J Magn Reson Imaging 5:165-170, 1995.

117. Murakami T, Kim T, Takamura M, et al. Hypervascular hepatocellular carcinoma: detection with double arterial phase multi-detector row helical CT. Radiology 218:763-767, 2001.

118. Muramatsu Y, Nawano S, Takayasu K, et al. Early hepatocellular carcinoma: MR imaging. Radiology 181:209-213, 1991.

119. Oudkerk M, Torres CG, Song B, et al. Characterization of liver lesions with mangafodipir trisodium-enhanced MR imaging: multicenter study comparing MR and dual-phase spiral CT. Radiology 223:517-524, 2002.

120. Paley MR, Ros PR. Hepatic metastases. Radiol Clin North Am 36:349-363, 1998.

121. Pauleit D, Textor J, Bachmann R, et al. Hepatocellular carcinoma: detection with gadolinium- and ferumoxides-enhanced MR imaging of the liver. Radiology 222:73-80, 2002.

122. Paulson EK, McClellan JS, Washington K, Spritzer CE, Meyers WC, Baker ME. Hepatic adenoma: MR characteristics and correlation with pathologic findings. AJR Am J Roentgenol 163:113-116, 1994.

123. Pawluk RS, Tummala S, Brown JJ, Borrello JA. A retrospective analysis of the accuracy of T2-weighted images and dynamic gadolinium-enhanced sequences in the detection and characterization of focal hepatic lesions. J Magn Reson Imaging 9:266-273, 1999.

124. Popper H. Pathologic aspects of cirrhosis. A review. Am J Pathol 87:228-264, 1977.

125. Quillin SP, Atilla S, Brown JJ, Borrello JA, Yu CY, Pilgram TK. Characterization of focal hepatic masses by dynamic contrast-enhanced MR imaging: findings in 311 lesions. Magn Reson Imaging 15:275-285, 1997.

126. Raman SS, Lu DS, Chen SC, Sayre J, Eilber F, Economou J. Hepatic MR imaging using ferumoxides: prospective evaluation with surgical and intraoperative sonographic confirmation in 25 cases. AJR Am J Roentgenol 177:807-812, 2001.

127. Regimbeau JM, Kianmanesh R, Farges O, Dondero F, Sauvanet A, Belghiti J. Extent of liver resection influences the outcome in patients with cirrhosis and small hepatocellular carcinoma. Surgery 131:311-317, 2002.

128. Reimer P. Tumor-targeted MR contrast agents: hype or future hope? Radiology 231:1-2, 2004.

129. Rodriguez-Bigas MA, Maamoun S, Weber TK, Penetrante RB, Blumenson LE, Petrelli NJ. Clinical significance of colorectal cancer: metastases in lymph nodes < 5 mm in size. Ann Surg Oncol 3:124-130, 1996.

130. Rofsky NM, Lee VS, Laub G, et al. Abdominal MR imaging with a volumetric interpolated breath-hold examination. Radiology 212:876-884, 1999.

131. Rohren EM, Turkington TG, Coleman RE. Clinical applications of PET in oncology. Radiology 231:305-332, 2004.

132. Rooks JB, Ory HW, Ishak KG, et al. Epidemiology of hepatocellular adenoma. The role of oral contraceptive use. Jama 242:644-648, 1979.

133. Ros PR, Ji H. Special focus session: multisection (multidetector) CT: applications in the abdomen. Radiographics 22:697-700, 2002.

134. Saini S, Stark DD, Hahn PF, et al. Ferrite particles: a superparamagnetic MR contrast agent for enhanced detection of liver carcinoma. Radiology 162:217-222, 1987.

135. Saini S, Reimer P, Hahn PF, Cohen MS. Echoplanar MR imaging of the liver in patients with focal hepatic lesions: quantitative analysis of images made with various pulse sequences. AJR Am J Roentgenol 163:1389-1393, 1994.

136. Salminen PM, Hockerstedt K, Edgren J, Scheinin TM, Tierala E. Intraoperative ultrasound as an aid to surgical strategy in liver tumor. Acta Chir Scand 156:329-332, 1990.

137. Samuel D, Figueiro J, Bismuth H. Liver transplantation: indication and patient selection. In: O´Grady JG, Lake JR, Howdle PD, ed. Comprehensive clinical hepatology. London: Mosby, 2000.

138. Schwartz LH, Seltzer SE, Tempany CM, et al. Prospective comparison of T2-weighted fast spin-echo, with and without fat suppression, and conventional spin-echo pulse sequences in the upper abdomen. Radiology 189:411-416, 1993.

139. Semelka RC, Simm FC, Recht M, Deimling M, Lenz G, Laub GA. T1-weighted sequences for MR imaging of the liver: comparison of three techniques for single-breath, whole-volume acquisition at 1.0 and 1.5 T. Radiology 180:629-635, 1991.

140. Semelka RC, Brown ED, Ascher SM, et al. Hepatic hemangiomas: a multi-institutional study of appearance on T2-weighted and serial gadolinium-enhanced gradient-echo MR images. Radiology 192:401-406, 1994.

141. Semelka RC, Willms AB, Brown MA, Brown ED, Finn JP. Comparison of breath-hold T1-weighted MR sequences for imaging of the liver. J Magn Reson Imaging 4:759-765, 1994.

142. Semelka RC, Schlund JF, Molina PL, et al. Malignant liver lesions: comparison of spiral CT arterial portography and MR imaging for diagnostic accuracy, cost, and effect on patient management. J Magn Reson Imaging 6:39-43, 1996.

143. Semelka RC, Worawattanakul S, Kelekis NL, et al. Liver lesion detection, characterization, and effect on patient management: comparison of single-phase spiral CT and current MR techniques. J Magn Reson Imaging 7:1040-1047, 1997.

144. Semelka RC, Balci NC, Op de Beeck B, Reinhold C. Evaluation of a 10-minute comprehensive MR imaging examination of the upper abdomen. Radiology 211:189-195, 1999.

145. Semelka RC, Cance WG, Marcos HB, Mauro MA. Liver metastases: comparison of current MR techniques and spiral CT during arterial portography for detection in 20 surgically staged cases. Radiology 213:86-91, 1999.

146. Semelka RC, Worawattanakul S, Noone TC, et al. Chemotherapy-treated liver metastases mimicking hemangiomas on MR images. Abdom Imaging 24:378-382, 1999.

147. Semelka RC, Helmberger TK. Contrast agents for MR imaging of the liver. Radiology 218:27-38, 2001.

148. Semelka RC, Martin DR, Balci C, Lance T. Focal liver lesions: comparison of dual-phase CT and multisequence multiplanar MR imaging including dynamic gadolinium enhancement. J Magn Reson Imaging 13:397-401, 2001.

149. Sherlock SD, Dooley J. Diseases of the liver and biliary system.London: Blackwell, 2002.

150. Shi M, Zhang CQ, Zhang YQ, Liang XM, Li JQ. Micrometastases of solitary hepatocellular carcinoma and appropriate resection margin. World J Surg 28:376-381, 2004.

151. Shuman WP, Baron RL, Peters MJ, Tazioli PK. Comparison of STIR and spin-echo MR imaging at 1.5 T in 90 lesions of the chest, liver, and pelvis. AJR Am J Roentgenol 152:853-859, 1989.

152. Smith FW, Mallard JR, Hutchison JM, et al. Clinical application of nuclear magnetic resonance. Lancet 1:78-79, 1981.

153. Smith FW, Mallard JR, Reid A, Hutchison JM. Nuclear magnetic resonance tomographic imaging in liver disease. Lancet 1:963-966, 1981.

154. Soe KL, Soe M, Gluud C. Liver pathology associated with the use of anabolic-androgenic steroids. Liver 12:73-79, 1992.

155. Solbiati L, Livraghi T, Goldberg SN, et al. Percutaneous radio-frequency ablation of hepatic metastases from colorectal cancer: long-term results in 117 patients. Radiology 221:159-166, 2001.

156. Solomon MJ, Stephen MS, Gallinger S, White GH. Does intraoperative hepatic ultrasonography change surgical decision making during liver resection? Am J Surg 168:307-310, 1994.

157. Soyer P, Levesque M, Caudron C, Elias D, Zeitoun G, Roche A. MRI of liver metastases from colorectal cancer vs. CT during arterial portography. J Comput Assist Tomogr 17:67-74, 1993.

158. Soyer P, Bluemke DA, Reichle R, et al. Imaging of intrahepatic cholangiocarcinoma: 2. Hilar cholangiocarcinoma. AJR Am J Roentgenol 165:1433-1436, 1995.

159. Soyer P, Gueye C, Somveille E, Laissy JP, Scherrer A. MR diagnosis of hepatic metastases from neuroendocrine tumors versus hemangiomas: relative merits of dynamic gadolinium chelate-enhanced gradient-recalled echo and unenhanced spin-echo images. AJR Am J Roentgenol 165:1407-1413, 1995.

160. Starzl TE, Francavilla A, Halgrimson CG, et al. The origin, hormonal nature, and action of hepatotrophic substances in portal venous blood. Surg Gynecol Obstet 137:179-199, 1973.

161. Tang Y, Yamashita Y, Namimoto T, Abe Y, Takahashi M. Liver T2-weighted MR imaging: comparison of fast and conventional half-Fourier single-shot turbo spin-echo, breath-hold turbo spin-echo, and respiratory-triggered turbo spin-echo sequences. Radiology 203:766-772, 1997.

162. Tang Y, Yamashita Y, Namimoto T, Takahashi M. Characterization of focal liver lesions with half-fourier acquisition single-shot turbo-spin-echo (HASTE) and inversion recovery (IR)-HASTE sequences. J Magn Reson Imaging 8:438-445, 1998.

163. Taylor HM, Ros PR. Hepatic imaging. An overview. Radiol Clin North Am 36:237-245, 1998.

164. Taylor M, Forster J, Langer B, Taylor BR, Greig PD, Mahut C. A study of prognostic factors for hepatic resection for colorectal metastases. Am J Surg 173:467-471, 1997.

165. Teefey SA, Hildeboldt CC, Dehdashti F, et al. Detection of primary hepatic malignancy in liver transplant candidates: prospective comparison of CT, MR imaging, US, and PET. Radiology 226:533-542, 2003.

166. Unger EC, Cohen MS, Gatenby RA, et al. Single breath-holding scans of the abdomen using FISP and FLASH at 1.5 T. J Comput Assist Tomogr 12:575-583, 1988.

167. Wallace JR, Christians KK, Quiroz FA, Foley WD, Pitt HA, Quebbeman EJ. Ablation of liver metastasis: is preoperative imaging sufficiently accurate? J Gastrointest Surg 5:98-107, 2001.

168. Wanless IR, Mawdsley C, Adams R. On the pathogenesis of focal nodular hyperplasia of the liver. Hepatology 5:1194-1200, 1985.

169. Ward J, Guthrie JA, Scott DJ, et al. Hepatocellular carcinoma in the cirrhotic liver: double-contrast MR imaging for diagnosis. Radiology 216:154-162, 2000.

170. Weg N, Scheer MR, Gabor MP. Liver lesions: improved detection with dual-detector-array CT and routine 2.5-mm thin collimation. Radiology 209:417-426, 1998.

171. Wei AC, Tung-Ping Poon R, Fan ST, Wong J. Risk factors for perioperative morbidity and mortality after extended hepatectomy for hepatocellular carcinoma. Br J Surg 90:33-41, 2003.

172. Whitney WS, Herfkens RJ, Jeffrey RB, et al. Dynamic breath-hold multiplanar spoiled gradient-recalled MR imaging with gadolinium enhancement for differentiating hepatic hemangiomas from malignancies at 1.5 T. Radiology 189:863-870, 1993.

173. Vogl TJ, Schwarz W, Blume S, et al. Preoperative evaluation of malignant liver tumors: comparison of unenhanced and SPIO (Resovist)-enhanced MR imaging with biphasic CTAP and intraoperative US. Eur Radiol 13:262-272, 2003.

174. World Health Organisation. Global estimates for health situation assessment and projections 1990. World Health Stat Q Spec No:1-51, 1990.

175. Yamashita Y, Fan ZM, Yamamoto H, et al. Spin-echo and dynamic gadolinium-enhanced FLASH MR imaging of hepatocellular carcinoma: correlation with histopathologic findings. J Magn Reson Imaging 4:83-90, 1994.

176. Yamashita Y, Hatanaka Y, Yamamoto H, et al. Differential diagnosis of focal liver lesions: role of spin-echo and contrast-enhanced dynamic MR imaging. Radiology 193:59-65, 1994.

177. Yamashita Y, Mitsuzaki K, Yi T, et al. Small hepatocellular carcinoma in patients with chronic liver damage: prospective comparison of detection with dynamic MR imaging and helical CT of the whole liver. Radiology 200:79-84, 1996.

178. Yeh CN, Chen MF, Lee WC, Jeng LB. Prognostic factors of hepatic resection for hepatocellular carcinoma with cirrhosis: univariate and multivariate analysis. J Surg Oncol 81:195-202, 2002.

179. Yoshida H, Itai Y, Ohtomo K, Kokubo T, Minami M, Yashiro N. Small hepatocellular carcinoma and cavernous hemangioma: differentiation with dynamic FLASH MR imaging with Gd-DTPA. Radiology 171:339-342, 1989.

180. Zacherl J, Scheuba C, Imhof M, et al. Current value of intraoperative sonography during surgery for hepatic neoplasms. World J Surg 26:550-554, 2002.